Quaternary Science Reviews 28 (2009) 1914–1931

Contents lists available at ScienceDirect

Quaternary Science Reviews

journal homepage: www.elsevier.com/locate/quascirev

OSL dating of the Aterian levels at Dar es-Soltan I (Rabat, Morocco) and implications for the dispersal of modern *Homo sapiens*

R.N.E. Barton [a,*], A. Bouzouggar [b], S.N. Collcutt [c], J.-L. Schwenninger [d], L. Clark-Balzan [d]

[a] *Institute of Archaeology, University of Oxford, 36 Beaumont Street, Oxford OX1 2PG, UK*
[b] *Institut National des Sciences de l'Archéologie et du Patrimoine, Rabat, Morocco*
[c] *Oxford Archaeological Associates Ltd, Oxford OX4 1LH, UK*
[d] *Research Laboratory for Archaeology & the History of Art, University of Oxford, Oxford, UK*

ARTICLE INFO

Article history:
Received 23 November 2008
Received in revised form
23 March 2009
Accepted 25 March 2009

ABSTRACT

The Aterian is a distinctive Middle Palaeolithic industry which is very widely spread across North Africa. Its dating and significance have been debated for nearly a century. Renewed interest in the Aterian has arisen because of a recent proposal that its development and spread may be linked to the dispersal of anatomically modern humans. The industry contains technological innovations such as thin bifacially flaked lithic points and pedunculates as well as evidence for personal ornaments and use of red ochre. Such markers as shell beads are believed to be indicative of symbolic behaviour. Dar es-Soltan I on the Atlantic coast of Morocco contains a thick sequence of Aterian deposits that were thought to represent the later stages of development of this industry. New Optically Stimulated Luminescence dates and geomorphological study indicate a much older sequence and so far the earliest yet recorded ages for the Aterian. They suggest an appearance in the Maghreb region during MIS (Marine Isotope Stage) 5.

1. Introduction

The age of the Aterian and its cultural significance in North Africa have been widely debated for almost a century. Following publication of the type site of Bir-el-Ater, Algeria (Reygasse, 1919–1920), the Aterian became recognised as a distinctive industry that could be traced across much of North Africa, stretching from the Atlantic coast to the Kharga Oasis and the fringes of the Nile Valley (Caton-Thompson, 1946). Despite unresolved issues about the application of terms like Mousterian, Middle Stone Age (MSA) and Middle Palaeolithic to the North African record there is still general agreement with the original idea that the Aterian is related to one of these complexes (Caton-Thompson, 1946; Ferring, 1975; Hublin, 1992; Debénath, 2000). However no such consensus exists about its geographical origins (see Garcea, 2004) or of the dating of its first appearance (Alimen et al., 1966; McBurney, 1967; Debénath et al., 1986; Tillet, 1995; Garcea, 2004). A recent suggestion proposes that its development and spread may be linked to the dispersal of behaviourally modern humans (McBrearty and Brooks, 2000). In this paper we present new OSL dates for Morocco that are the earliest yet recorded for this industry and suggest a development in the Maghreb region during MIS (Marine Isotope Stage) 5.

2. The problems of dating the Aterian

In her seminal paper on the Aterian Caton-Thompson (1946) described finds from a wide number of locations across North Africa that shared characteristics of a 'Levalloiso-Mousterian' lithic technology 'without true blade elements' and with tools that included distinctive tanged or pedunculate points and bifacially worked leaf-shaped forms (1946, p. 106). Such artefacts had been collected from various locations in North West Africa from the nineteenth century onwards (Moreau, 1888; Morgan et al., 1910; Debruge, 1912) but had rarely been reported from *in situ* contexts. A potential exception was that of Carrière (1886) who recorded stratified finds from Eckmuhl Cave in the Oran region of Algeria. Further fieldwork in the 1930s yielded stratigraphic evidence that placed the Aterian in relation to the Mousterian (Breuil and Frobenius, 1931) and this led to the adoption of a sequence by French archaeologists that has remained more or less unchanged to the present day (Hublin, 1992). Various sub-divisions of the Aterian that were thought to be of chronological significance were also recognised in this early period but were based largely on lithic typology (Antoine, 1937; Ruhlmann, 1939).

Thus the earliest understanding of the Aterian chronology rested upon typological and stratigraphic comparisons and, in Morocco, the relationship of archaeological deposits to marine terraces. Early geological surveys were undertaken by Lecointre

* Corresponding author. Tel.: +44 01865 278240; fax: +44 01865 278254.
E-mail address: nick.barton@arch.ox.ac.uk (R.N.E. Barton).

0277-3791/$ – see front matter © 2009 Elsevier Ltd. All rights reserved.
doi:10.1016/j.quascirev.2009.03.010

(1926) and by Neuville and Ruhlmann (1941). These authors were able to show that the sequence of Aterian occupation of caves along the Moroccan coast could be understood with reference to a four-stage succession of high sea level stands. This placed the Aterian after the 'last great pluvial' ("Würm I"), with caves such as El Khenzira and Dar es-Soltan created by marine transgressions of a higher sea level (Ruhlmann, 1936, 1951). Dar es-Soltan itself became the type site of the last 'glacial' period known as the Soltanian (Choubert, 1953; Choubert et al., 1956).

With the availability of the radiocarbon technique a number of Aterian sites in Morocco were dated using this method (Roche, 1976). Although the sample of sites was relatively restricted it was possible to demonstrate 'infinite' ages for this industry at Taforalt (Roche, 1976) and at Dar es-Soltan I (Debénath et al., 1986). The end of the Aterian was suggested to be around 24 500 ± 600 BP (Gif 2582) and 23 700 ± 1000 BP (Gif 2585) at Contrebandiers (Témara) although other even younger radiocarbon dates from this site were rejected (Debénath et al., 1986). As a result in the 1980s there was a general accord amongst the majority of scholars that the Aterian occupied the interval from around 40 ka BP to 25–20 ka BP (Debénath et al., 1982).

The first luminescence dates relevant to the Aterian were published by Debénath et al. (1986). Using Thermoluminescence (TL) a date of 41 160 ± 3500 BP (BOR 56) was recorded for the cave of El Harhoura I (Témara) and both TL and the relatively new Optically Stimulated Luminescence (OSL) methods were used at Chaperon-Rouge I (Texier et al., 1988). These placed the habitation floor at 28 200 ± 3300 (OX TL 724g) with the capping of aeolian sands at 24 000 + 3050/−4800 (OX OSL 724g2), which fitted the existing radiocarbon chronology. However, more recent luminescence studies have pushed the initial Aterian presence much further back in time for other parts of North Africa. For example, TL and OSL dates from the Tadrart Acacus in SW Libya have revealed stratified Aterian artefacts in layer 22 of Uan Tabu rockshelter dating to 61 ± 10 ka (Cremaschi et al., 1998), while "supposedly Aterian artefacts" from Uan Afuda provided two TL ages of 70.5 ± 9.5 and 73 ± 10 ka, and OSL ages ranging from 69 ± 7 ka for the artefactual levels to 90 ± 10 ka from the underlying sands (Martini et al., 1998; Garcea, 2004). In Tunisia, at Oued el Akarit, a 'proto-Aterian' with pedunculates is dated by TL to 90 ka (Roset, 2005), whilst in Morocco, in the first well-documented stratigraphic succession between the Mousterian and Aterian, work at Rhafas Cave in Morocco has suggested an age of between 70 and 80 ka for the earliest Aterian (Mercier et al., 2007). These authors report the latest Mousterian comes from level 3b dating to around 80–90 ka and thus can be attributed to late MIS 5 (Mercier et al., 2007, p. 312). In the OSL, TL, and U-series dates at Grotte des Pigeons, Taforalt, Morocco, the earlier Aterian levels lie between 73 and 91 ka (Bouzouggar et al., 2007a). Other Uranium-series dates on tufas and carbonates in Egypt (Szabo et al., 1995; Smith et al., 2007), and ESR dates on tooth enamel in Aterian layers at Mugharet el'Aliya, Morocco (Wrinn and Rink, 2003) support the older chronology suggested by luminescence dating.

The emerging picture of a much older origin for the Aterian also arises out of scepticism relating to the application of conventional radiocarbon techniques. In particular, it is clear that many of the early radiocarbon measurements were made on bulked charcoal or bone (Barton et al., 2007) while at Taforalt some of the oldest dates were based on shell and were thus susceptible to the effects of secondary carbonate contamination, as noted at Contrebandiers, Dar es-Soltan II and El Harhoura I (Occhietti et al., 1993). Other problems stem from the uncertainty of the original archaeological associations at sites like Contrebandiers and there was often a lack of attention given to the meaning of infinite ages that were obtained from Aterian archaeological layers (Garcea, 2004).

Linked with a general dissatisfaction with the younger chronology is a renewed focus of interest on human fossils in the Aterian. According to recent work on dental remains from Contrebandiers, El Harhoura and Dar es-Soltan II, growth and morphological patterns of the teeth are consistent with modern humans (Hublin et al., 2007), although this is a view that is not shared by all (e.g. Trinkaus, 2007). Similarly, fresh studies of the archaeological evidence have linked the Aterian with the precocious appearance of symbolic ornaments such as perforated shell beads and ochred finds (Bouzouggar et al., 2007a), as well as bone tools (El Hajraoui, 1994) and structured hearths and living spaces (Nespoulet et al., 2008; Debénath et al., 1986). A similar combination of traits has also been noted in the MSA of southern Africa where technological and behavioural innovation have been recognised in the Still Bay complex dating to between 70 and 80 ka (Henshilwood et al., 2002; Jacobs et al., 2008a) and is accepted by many authors as unequivocal evidence of early symbolic behaviour spread by modern humans (Wadley, 2001; Bar-Yosef, 2002; Henshilwood and Marean, 2003; D'Errico and Henshilwood, 2007). On the other hand, for North Africa it has been argued that the Aterian is a relatively late cultural development and therefore is of only marginal importance to the evolution and early spread of modern humans (Trinkaus, 2007).

Despite these new advances, there are still relatively few well-dated Aterian sequences and it is obvious that secure chronological data are vital to underpinning arguments regarding the nature and development of this industry and its implications for understanding modern human expansion in North Africa. For example, if the Aterian is an archaeological marker for the dispersal of modern *Homo sapiens* (McBrearty and Brooks, 2000) then it would be important to compare the timing of its appearance in North West Africa to see if there was a direction of influence across the Sahara (Watson et al., 1997; Van Peer, 1998; Osborne et al., 2008), or from the south as originally hypothesised by Caton-Thompson (1946, p. 106). Equally, it would be crucial to determine whether climatic factors played a major role in the distribution of the Aterian and whether this might have been related to the opening of corridors through the Sahara during more humid episodes of MIS 5 (132–74 ka) as has been suggested by some authors (Garcea, 2004; Garcea and Giraudi, 2006; Osborne et al., 2008). It is for these reasons that the new dating of the sequence of Aterian deposits at Dar es-Soltan I assumes special significance.

3. Dar es-Soltan I

Dar es-Soltan I (DeS I) is one of several caves opening from a low calcarenite cliff on the Atlantic coast of Morocco near Rabat (33°58′44″N, 6°53′51″W) (Fig. 1). The cave entrance faces west (300° magnetic), towards the ocean, with the modern shoreline nearly 260 m distant. The cave is at least 43 m deep and more than 6 m wide, with a thickness of at least 8 m of deposits throughout (Ruhlmann, 1951).

Excavation of DeS I was carried out by Dr. Armand Ruhlmann of the *Inspection des Antiquités du Maroc*. Two expeditions occurred in 1937 and in 1938, though tragically Ruhlmann died in 1948 following an accident in El Aïoun in eastern Morocco before his work could be fully written up. The posthumous 1951 account of '*La Grotte Préhistorique de Dar es-Soltan*' was based on his copious excavation notes and was compiled and published under the direction of Henri Terrasse of the *Institut des Hautes Etudes Marocaines*.

In the monograph a 7.5 m sequence of deposits is described extending from assumed bedrock to the roof of the cave. Ruhlmann's stratigraphic section of the cave deposits (see Fig. 2) comprised 12 Layers (M–A), with a major rock fall shown between

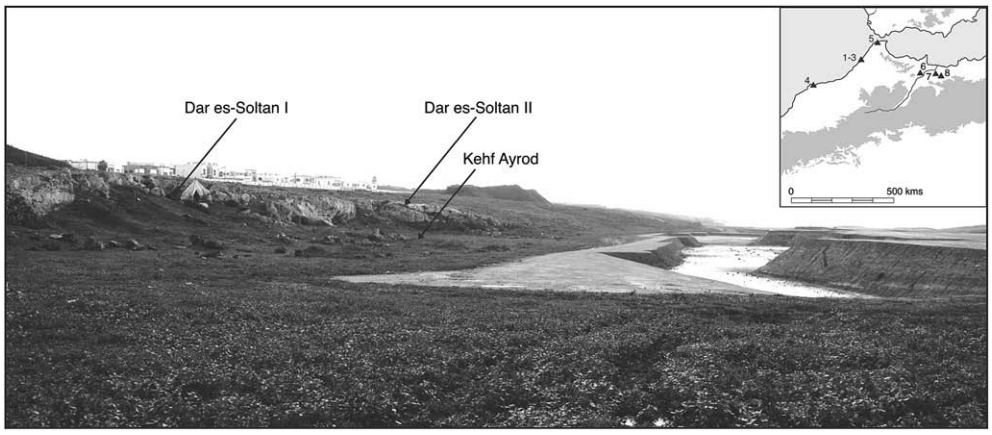

Fig. 1. General location of Dar es-Soltan. Inset map 1–3: Dar es-Soltan I–II, El Mnasra, and Contrebandiers; 4: El Khenzira; 5: Mugharet el Aliya; 6: Ifri n'Ammar; 7: Taforalt; 8: Rhafas. The photograph from November 2009 shows the view south with extensive construction workings outside the caves in the inter-dunal area and the fossil dune overlooking the present-day beach platform.

Layers C and B. According to him the sequence contained three discrete Aterian archaeological layers separated by sterile deposits and overlain by a Neolithic layer near the summit. The main archaeological 'units' were described as *Foyers Archéologiques* (clearly meaning 'hearth-rich layers'). The Aterian industries comprised an *Atérien inférieur* (Lower Aterian), near the top of Layer I, an *Atérien supérieur* (Upper Aterian), at the base of Layer C (C2), and a *Moustérien décadent* (Devolved Mousterian) situated at the top of Layer C (C1). The extensive Neolithic layer was situated above the rock fall and was made up of a 1.5 m shell midden (B), apparently capping the majority of the cave deposits, with 0.5 m of stony grey deposits (A) immediately above that.

3.1. Aterian artefact assemblages

The artefacts from the lowest Aterian assemblage (I) were recorded as coming from a 30 cm thick horizon. According to Ruhlmann, from a total collection of 248 lithic artefacts in the assemblage, 29 pedunculate tools were described including two end scrapers on tanged supports. He also noted the presence of side

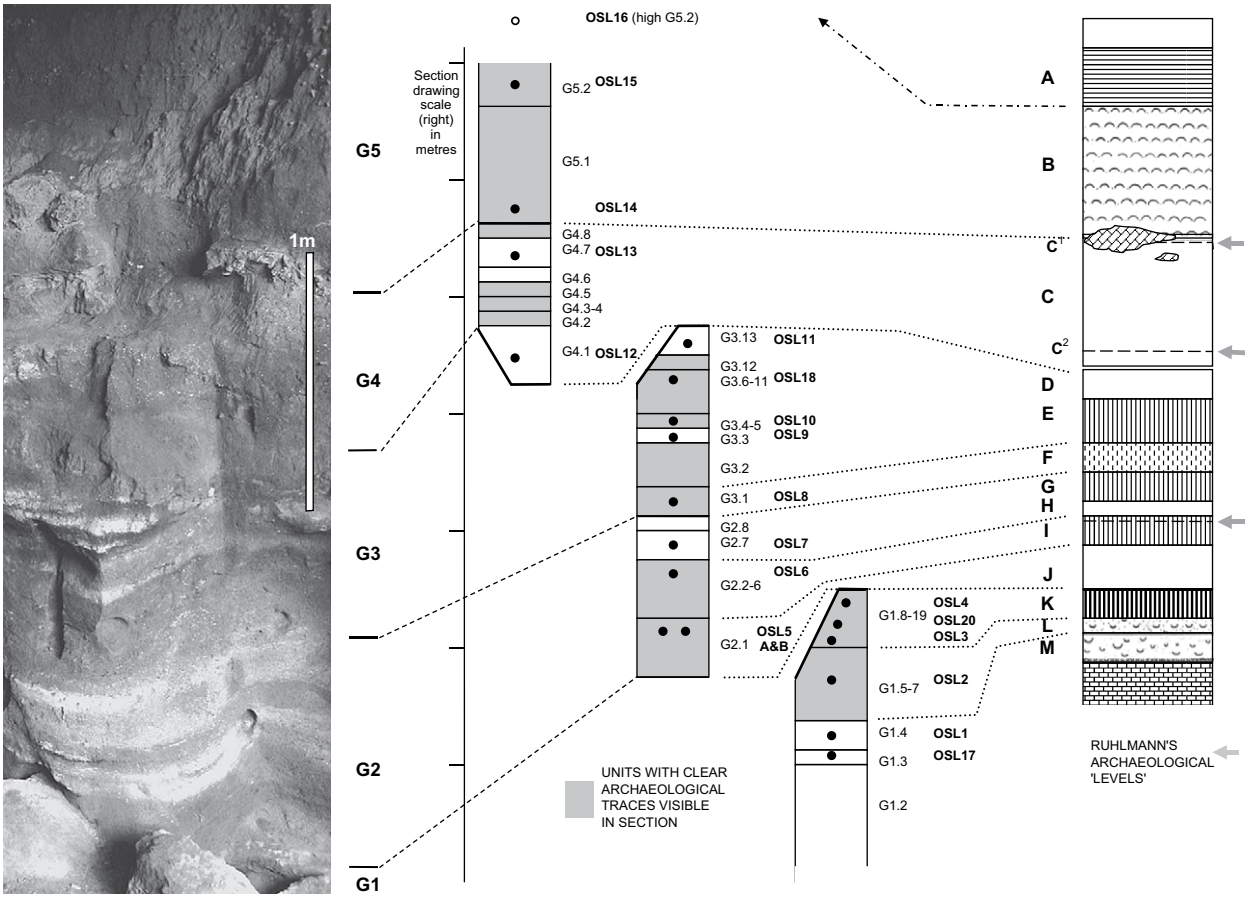

Fig. 2. Composite section showing location of OSL samples collected from the exposed sediment sequence inside the cave of Dar es-Soltan I.

scrapers and typical Levallois flakes and cores in the assemblage. The raw material consisted predominantly of siliceous rocks (90%) with the rest of the artefacts made up of quartzite, sandstone, schists and diorites and a unique example of a flake in hematite (Ruhlmann, 1951, p. 6). Two ivory objects, one shaped like a point and the other a small *plaquette* were also attributed to this group.

Approximately 1.5 m of sterile deposits separated the lowest Aterian assemblage from a second situated in the lower 20–30 cm of C2. This overlying industry was again typified by the presence of Levallois flakes and cores and a range of retouched tools such as side scrapers. Amongst the assemblage of 185 artefacts Ruhlmann noted that, in addition to pedunculate pieces (33) and end scrapers (2), there were foliate pieces, three of which he styled as '*feuille de laurier*'. The more evolved features of this assemblage included a burin.

A third layer was described by Ruhlmann near the top of Layer C which he called C1. It consisted of 95 artefacts, all of fine-grained chert and quartzite. Although flakes with faceted butts were present the Levallois component was much reduced. No tanged points were reported, but amongst the tools were small geometrics. He suggested that the local Aterian had in some senses returned to a *Moustérian primitif* and coined the term *Moustérian décadent* (literally 'degenerate' or 'devolved' Mousterian) for the cultural attribution of this layer. Since no corresponding industry had been noted elsewhere in the region, he supposed it to have been a purely local development.

3.2. Re-assessment of the Ruhlmann sequence

A re-examination of the cave sequence was undertaken in June 2005 by four of the authors (NB, AB, SC & J-LS) during which the sediments were described and samples for dating were taken. Professor André Debénath and Dr Roland Nespoulet were also present for some of the time. A further set of relevant observations were made (by NB, AB, SC & J-LS) in November 2008, during a visit to the site to obtain microtephra, palaeoenvironmental and further dating samples, as part of the continuing programme of research at the site by the UK–Morocco project.

3.2.1. Lithostratigraphic description

The following composite sedimentary log was recorded in various vertical segments spaced, according to clarity of exposure, along approximately 6 m of longitudinal sections left by Ruhlmann. As a temporary lithostratigraphic system, the sequence has been divided into five 'Groups' (broadly of 'member' lithostratigraphic rank), based upon significant sedimentological differences and major erosional events or unconformities. The correlation with Ruhlmann's stratigraphy (with units marked '(R)' below) is usually clear (see also Fig. 2).

3.2.2. Lithogenesis and constraints on regional correlation

The regional context of the DeS I deposits constrains and qualifies discussion of the chronological framework. The Atlantic coast of Morocco, especially in the zones around Rabat and Casablanca, has been the subject of repeated chronostratigraphic syntheses. The most recent and reliable review has been given by Texier et al. (2002) and Lefèvre and Raynal (2002), with chronometric dating (OSL) reported by Rhodes et al. (2006). The younger end of this succession is of interest here and may be summarised, from oldest to youngest (Tables 1 and 2).

Each of the marine intervals is interpreted as transgressive, lying directly upon an erosion plane cut across bedrock (usually pre-Quaternary basement in the Casablanca area) and notched into the units of the preceding (higher) cycle, in the manner of a 'staircase' rising inland. There are additional red beds (interpreted as colluvium and stable palaeosols), both within dune sequences and in the slacks between ridges.

Looking first at the marine, broadly 'interglacial', intervals, the suggested correlation with the global marine isotopic record[1] can furnish a more accurately dated sea level curve for the Casablanca area.

It would appear, from particularly tectonically stable regions, that interglacial maximum sea levels have not differed greatly from the present level over much of the Pleistocene. For instance, Murray-Wallace (2002) reviews data from southern Australia, where fossil shorelines can often be traced horizontally over hundreds of kilometres, concluding that, for at least the past eleven interglacials, sea level highstands did not deviate by more than about 6 m from the present level, with MIS 5.5 falling in the bracket 2–6 m above present mean sea level. Studies of cores from the Red Sea are generally considered to provide more accurate sea level estimates (based mainly upon oxygen isotope composition) than is the case in more 'open' basin cases. Siddall et al. (2003, 2007) suggest that their sea level data are accurate to within ±12 m over a timescale of 470 ka and at centennial scale resolution; they note that the MIS 5.5 peak was not significantly higher than the present sea level, and that the 5.3 and 5.1 peaks were at least 15 m below that of 5.5. Recent data from the Barbados fossil reefs (Potter et al., 2004; Schellmann et al., 2004) again suggest that, after MIS 5.5, sea level did not rise above approximately −15 m (relative to current sea level, the best available adjustment having been made for steady uplift). Furthermore, on the basis of coherent sets of both uranium-series and ESR dates, there appear to have been more than one peak within each of the three 'classic' transgressive substages of MIS 5. Thus, according to these indicators, sea level reached its interglacial maximum during MIS 5.5.3 and MIS 5.5.2 between 132 and 128 ka. Subsequently, in MIS 5.5.1, sea level declined reaching a level of −11 m by ca 118–120 ka. During substage 5.3 sea level was always lower than in substage 5.5; it reached relative maxima at −13 m, −20 m and −25 m during MIS 5.3 (grouped around 105 ka) and formed three distinct coral reef terraces probably in relatively short time intervals. A double sea level oscillation is recognised during MIS 5.1, an early 5.1.2 interval (ca 85 ka) with a sea level at −21 m, and a late 5.1.1 interval (ca 74 or 77 ka) with a sea level at −19 m. In the Bahamas, a similar picture is emerging. Hearty and Neumann (2001) report that, early in MIS 5.5 (132–125 ka), the sea maintained a level of +2.5 m. A mid-5.5 regression around 124 ka is well documented, followed by a new rise to a slightly higher level than the previous one, allowing reef growth to a maximum elevation of less than +3 m. This near stillstand was short-lived, however: at the end of the period (towards 118 ka), sea level rose perhaps to +6 or +8.5 m. The subsequent fall to the substage 5.4 lowstand was rapid. Siddall et al. (2007) give additional data from around the world, showing a generally consistent picture. Even along the southern Spanish coast, multiple highstands within each MIS 5 substage have been reported (cf. Zazo et al., 2000). A similar pattern is also beginning to appear with respect to MIS 7 (ca 190–245 ka), for which a five-part main substage structure has also been identified, although apparently with much less amplitude variation than in MIS 5, each of the three MIS 7 sea level peaks reaching similar altitudes; a late, 'post-MIS 7', event is also recognised, in Barbados (Thompson and Goldstein, 2005) and in the Bahamas (Henderson et al., 2006), at ca 185 ka, but the sea level did not then rise higher than −15 m.

[1] The decimalised system of substage notation will be used in the present text for clarity; thus "MIS 5.5.1" is equivalent to the youngest high stand recognised in "MIS (formerly OIS) 5e", for example.

Table 1
Description of lithostratigraphy of Dar es-Soltan I.

Unit	Description
G5 (R)A (ca 0.65 m)	Group 5 – grey stony material (not yet observed in detail).
G5.1–2 (R)B (>2.5 m)	Group 5 – midden and fine sand. [G5.2] true midden; powdery, ashy, 5YR 4/2 and greyer upwards; strong marine shell bands, shell and charcoal increasing upwards; >1.5 m thick [**OSL 15-X2391** at 0.15 m from the base in cave interior on southern side; **OSL 16-X2392** in higher grey deposits on the northern side of the main entrance]. Near the entrance, on the north side of the Ruhlmann excavations, the base of G5.2 includes quite deep pits (in places cutting right through G5.1 and passing down into G4 by at least 50 cm). [G5.1] loamy fine sand; almost homogeneous in places but with subtle layering (including some laminated intervals) in less leached zones; not well compacted and practically no point cementation; 5YR 6/6 (orangey) at base, grading continuously upwards to 5YR 6/3 (i.e. losing chroma); burrows; common groups of land mollusca; increasing marine shells upwards; rare artefacts including a backed bladelet and charcoal specks, especially at approximately mid-height; 0.96 m thick [**OSL 14-X2390** at 0.25 m above base].
G4.1–8 (R)C (ca 1.3 m)	Group 4 – upper red-brown units, all dense and well consolidated; strong gullying throughout but especially at the base, apparently water entering from southern and especially the eastern openings; more or less pronounced trough bedding at most levels; very large slabs (up to 0.3–0.4 m thick 1.0–1.5 m long) at all levels in G4 in the back of the cave but then only towards top, and eventually disappearing, westwards out of cave, plausibly derived from the east (collapse eventually leading to the wide opening present today). [G4.8] [probably equivalent to (R)C[1]]: red-brown powdery loam; some stone blocks; common concretions, some very strong, either as globules or thin platelets, phosphates probably included; thin but strong carbonate crust at top; burnt specks and charcoal flecks; 0.13 m thick. [G4.7] light red-brown (7.5–10YR 5/3) very silty loam; increasing white concretions upwards, becoming almost cemented at top; originally finely laminated but disturbed by small-scale bioturbation; 0.16 m thick [**OSL 13-X2389**]. [G4.6] light brown silty loam; small concretions strengthening upwards; 0.10 m thick. [G4.5] rather chaotic powdery loam with fine sand but with some silty trough-form lenses; common flecks (often angular clasts) of pure (no included sand grains), white material (probably roof/wall speleothem fragments also with an outside possibility of some reworked exterior calcrete fragments); burnt stone, charcoal; small-scale bioturbation; 0.19 m thick. [G4.4] [possibly equivalent to (R)C[2]]: dark brown powdery loam with fine sand; charcoal flecks; small-scale bioturbation; 0.06 m thick. [G4.3] uniform mid-brown (7.5YR 5/3) powdery loam with fine sand; small-scale bioturbation; 0.09 m thick. [G4.2] massive dark brown (5YR 3/2) powdery loam with fine sand, with white speckles; continuous across the top of troughs G4.1; lithic chips; small-scale bioturbation; 0.11 m thick. [G4.1] erosion troughs at the base of G4, poor bedding, generally light brown material with eroded concretions; trough orientation is down towards 340° mag; individual troughs 0.40–0.50 m thick [**OSL 12-X2388** in eastern transverse section].
G3.2–13 (R)D (R)E (ca 1.4 m)	Group 3 – roughly horizontal beds throughout cave (lacking significant cross-dip); across (seen in E–W section) the entrance below the southern opening, gentle domed form (local low talus); darker brown with carbonate beds; common charcoal, true hearth lenses, artefacts; somewhat truncated by gullying in places. The darker units in G3 (interpreted as dominated by hearths and/or hearth cleanings) are generally cyclic [top: light (ash and carbonate); pink (fired), black (charcoal), dark brown (charcoal flecks and powder), brown (mineral)], the motif being recognisable in any single vertical line but the units appearing as lenses over several metres horizontally. [G3.13] [probably equivalent to (R)D]: powdery loam with fine sand, 7.5YR 4/2–3; small concretions only but with strong overall carbonate content; extremely diffuse bedding in places only, otherwise massive; capped by an irregular (gullied) contact, annealed; 0.27 m thick [**OSL 11-X2387** in eastern transverse section]. [G3.12] [G3.7–12 possibly equivalent to part of (R)E]: mid-brown material, with dark (charcoal) and light (carbonate) 'streaks'; bioturbation; 0.18 m thick. [G3.11] light material; carbonates; bioturbation, generally small-scale but becoming extreme; 0.08 m thick [**OSL 18-X2394**]. [G3.10] dark material; charcoal; 0.03 m thick. [G3.9] light material; carbonates; 0.03 m thick. [G3.8] dark material, black at top; pink to orange burnt flecks and small patches; 0.08 m thick. [G3.7] [light material; carbonates; 0.02 m thick]. [G3.6] [G3.2–6 probably equivalent to part of (R)E]: dark material, almost black in places, especially near the top; extremely common charcoal; bioturbation (including forms resembling insect burrows); 0.08 m thick. [G3.5] very thin and discontinuous 'cream' concretion line; 0.01 m or less thick. [G3.4] dark material with a little more medium sand; very common charcoal, at least two hearth lens intervals; bioturbation (including forms resembling insect burrows); 0.20 m thick [cf. **OSL 10-2386**]. [G3.3] light (creams to light oranges) gritty loam, 7.5YR 7–8/3; carbonate-rich, possibly originally containing some discontinuous floor speleothem (now decomposed); very strong small-scale bioturbation (including forms resembling insect burrows), breaking up the layer in places; 0.07 m thick [**OSL 9-X2385**]; the carbonate band is traceable over much of the section, becoming thicker, and with increasing orangey sand loam beneath, westwards out of cave. [G3.2] powdery sandy loam, similar to G3.1 below, but only rare concretions (clean face easy to cut); diffuse bedding traces (2–3 cm thick); bioturbation; lithic artefacts in section; common dispersed charcoal; clear 6–7 cm thick hearth traceable over at least 100 cm laterally, black at base, thin pink (fired) lens, grey/cream ash/carbonate at top; unit 0.32 m thick overall. Further west, broad 'swells' develop in the section at this level, an effect that becomes stronger upwards through G3; these forms appear to be due to delta-like feeds from the southern opening.
G3.1 (R)F (ca 0.3 m)	Group 3 – carbonate-rich facies. [G3.1] powdery sandy loam, 7.5YR 3/3 to 4/2; extremely common small concretions and eucladioliths, more discrete lens of eucladioliths near the top; generally 'granular/crumb/nodular' texture due to concretions (not possible to cut a clean face); poor bedding, slight dip (5°) at least locally westwards out of cave; generally bioturbated with common burrows, some quite large (note also 15 cm width recent burrows with strong red-brown fill); very common dispersed charcoal, fragments up to 1 cm diameter, possible hearth lens at eastern end of section; 0.28 m thick [**OSL 8-X2384**].
G2?.8 (R)G (ca 0.1 m)	Possibly Group 2. [G2?.8] silty sandy loam, various browns; diffuse bedding but some clear laminations; darker brown uppermost, some concretions in centre, lighter brown below; strong small-scale bioturbation, with a very irregular (burrowed) upper contact; cut out westwards before southern opening; 0.12 m thick.
G2.7 (R)G&H (ca 0.3 m)	Group 2; banded sediments, rising gently into cave (but low amplitude long wavelength wavy); apparently quite strong cross-dip (down to the south or southeast); includes quite strong carbonate layers, some decayed but true discontinuous stalagmite; some charcoal and bone present; truncated by angular unconformity. [G2.7] [probably equivalent to parts of (R)G&H]: sandy loam; colours generally from 5YR 4/5 to 7.5YR 5/6; rather massive, light brown lenses but generally only very diffuse bedding; common white concretions (apparently mostly fallen speleothem fragments and eucladiolith masses), quite large in places; stronger *in situ* concretions at top of unit (light browns/creams 7.5YR 6–7/3), getting stronger eastwards into the cave, including a true stalagmite root; small-scale bioturbation; 0.33 m thick [**OSL 7-X2383**].

Table 1 (*continued*)

Unit	Description
G2.2–6 Mostly (R)I (ca 0.4 m)	Group 2 – banded sediments, rising into cave (but low amplitude long wavelength wavy); almost horizontal at S3, westerly dip increasing inwards from ca 5° to 12°–18°; apparently quite strong cross-dip (down to the south or southeast); includes relatively strong carbonate layers, some decayed but true discontinuous stalagmite; some charcoal and bone present. [G2.6] markedly silty loam with fine sand; 7.5YR 3–4/4, a little more orange at base; internal bedding not very clear; rare small concretions; common small-scale bioturbation, apparently penecontemporaneous; common charcoal flecks; hearth (cf. **OSL 6-X2382**) at approximately mid-level in this unit, such that material above this may correlate with (R)H; 0.18 m thick. [G2.5] derived eucladiolith unit; eucladioliths grouped in gently domed and even bifurcating lenses (interpreted as due to shifting depocentres); diffuse lamination; strong and continual small-scale bioturbation (roots, mollusca and insects, amorphous chambers and tubes 3–20 mm in diameter), at least partially penecontemporaneous; 0.06 m thick. [G2.4] earthy material with common fine sand; dark (7.5YR 4/4, possibly some charcoal powder; diffuse lamination; strong bioturbation; 0.05 m thick. [G2.3] light material with derived eucladioliths and tiny speleothem platelets, eucladioliths grouped in gently domed and even bifurcating lenses (interpreted as due to shifting depocentres); 7.5YR 7/3 to 6/4 but rather blotchy; diffuse lamination; small-scale bioturbation (roots, mollusca and insects, amorphous chambers and tubes 3–20 mm in diameter), at least partially penecontemporaneous; some burnt bone fragments; 0.09 m thick. [G2.2] intermittent *in situ* carbonate crust, very hard and well lithified; 0.01 m thick.
G2.1 (R)J (ca 0.5 m)	Group 2; banded sediments, rising gently into cave (but low amplitude long wavelength wavy); includes quite strong carbonate layers; some charcoal and bone present. [G2.1] relatively plastic (clayey) sandy loams, with an 'average' colour of 7.5YR 4/3–4; lighter beds are sandier (7.5YR 5/4 speckled lighter at sandiest), bands of darker (7.5YR 3/3 plus black streaks) clayier material with Mn and common charcoal; carbonates generally corroded but eucladioliths present towards the top; rare small corroded stones; reasonably well laminated, 5–10 mm thick sets, more or less horizontal in N–S plane, roughly horizontal in outer part but further into cave dipping 5°–8° westwards out of cave; common minor bioturbation (insect/mollusc channels, roots, including some modern); lithic artefacts at least two levels (**OSL 5A&B-X2380/1**, with several lithic artefacts and bones, probably from near the top of this unit); 0.51 m thick; thinning (base rising above unconformity) westwards out of cave; eastwards and northeastwards into cave, this unit on-laps the again rapidly rising unconformity capping G1.
G1.8–19 (R)K (>0.6 m)	Group 1 – well bedded (probably originally laminated at most levels), concreted (harder into cave), strongly variegated units, with common 'chocolate' Mn colours, bedded dipping down (12°) towards the west (towards the main entrance); truncated by angular unconformity, dipping down (12°) into cave, itself cemented/welded. [Probably additional higher units westwards, cut out by unconformity in the exposed section.] [G1.19] concreted sandy clay loam; strong orangey with dark streaks; 0.04 m thick. [G1.18] cream-coloured carbonate band; 0.02 m thick. [G1.17] concreted sandy clay loam; orangey brown; 0.04 m thick. [G1.16] cream-coloured carbonate band; 0.02 m thick [**OSL 4-X2379** centred at this level]. [G1.15] concreted sandy clay loam; brown with dark streaks; bioturbation pouches reaching down into underlying unit; 0.04 m thick. [G1.14] concreted sandy clay loam; orangey and mid-brown, light brown where carbonates stronger; 0.06 m thick. [G1.13] concreted sandy clay loam; very dark brown to black, with flecks of charcoal; shallow bioturbation pouches cutting top of underlying unit; 0.04 m thick. [G1.12] cemented sandy clay loam; light brown to orangey; carbonates at base; 0.07 m thick. [G1.11] weakly concreted sandy clay loam; dark brown, with darker streaks; lithic artefacts; 0.07 m thick. [G1.10] concreted sandy clay loam; laminae of brown, orangey, cream-colour, dark partings; 0.04 m thick [**OSL 20-2396** centred on this unit]. [G1.9] carbonate band, possibly some true floor speleothem in places; white/yellow/cream; 0.03 m thick. [G1.8] concreted sandy clay loam; light brown to strong orangey; 0.10 m thick [**OSL 3-X2378**].
G1.5–7 (R)L (ca 0.6 m)	Group 1 – coarser sands (disturbed/reworked upper units). [G1.7] moderately well cemented, recrystallised sand; probably laminated, reasonably uniform overall, dip consistent with the set above; 5YR 3/3 with some more orangey patches; lighter grey 'clayey' lens at mid-height, with charcoal and lithic artefacts; 0.23 m thick [**OSL 2-X2377** towards base] [G1.6] heavily cemented sand, losing bedding forms during the nodular concretion process; still some clay in the matrix; relatively dark grey brown; 0.12 m thick. [G1.5] heavily cemented beach rock; greyish; 0.23 m thick (graded base).
G1.1–4 (R)M (>1.1 m)	Group 1; coarser sands. [G1.4] patchily cemented (merging nodules), medium to coarse, poorly bedded shelly sand; some Mn-stained microvertebrate bones; light orange 7.5YR 6/6 speckled white; lower boundary shows load structures 3–4 cm in vertical extent; 0.20 m thick [**OSL 1-X2376** at mid-height]. [G1.3] patchily cemented (merging nodules), light (7.5YR 7/3 speckled white), very well laminated (planar) shelly sand; stringers of shell; including *Patella*, *Mytilus*, *Nassarius*, *Cardium* and 'whelks', with some quite large specimens; 0.15 m thick [**OSL 17-X2393** in upper part of this unit]. [G1.2] [probably not reached by Ruhlmann, mistaken for bedrock]: patchily cemented (merging nodules), light orangey coarse sand; quite well bedded; darker stringers; shelly; >0.70 m thick. [G1.1 Undefined – to represent any underlying sand units not yet exposed.]
Bedrock	[**OSL 19-X2395** from a weathered fallen block in the eastern transverse section; **OSL 21-X2397** from an exterior aeolianite bedrock exposure south of the cave.]

The significant points here are that, in each 'odd-numbered' stage, sea level reached altitudes as high as or even slightly above modern values, in MIS 5.5 during the interval 118–132 ka and in MIS 7.1 during the interval 190–198 ka (and also during earlier MIS 7 peaks). At all other times, including later substages of MIS 5 and the 'post-MIS 7' event, sea level remained at least 15 m below modern values.

Returning to the Moroccan coast near Casablanca, the entire Pleistocene sequence suggests relatively steady uplift, perhaps with some rate variations through time but with an average of no more than 0.45 m per 10 ka and no identified reversals of trend. It follows that, in most if not all cases, there would be insufficient time for any marine deposits formed during the −15 m secondary peaks of 'later' substages to be uplifted beyond the reach of the next main transgression (MIS 7.1, MIS 5.5 and MIS 1). Even if some such 'later' substage deposits had survived erosion, anything post-dating MIS 7 would still lie below modern sea level. Assuming that the neotectonic model holds along the morphologically quite uniform coast north and south of Casablanca, it would be most unlikely that marine deposits from any other periods than the main highstands will survive. This proposition appears to be borne out by observation, with no reports of, say, post-MIS 5.5 marine deposits in the literature on the Rabat–Casablanca coast before the onset of MIS 1. An apparent contrary case in the general vicinity (north of Rabat), in which two marine cycles have been attributed to MIS 5.5 and MIS 5.3 (Plaziat et al., 2006), is either a special geomorphological setting or might give rise to the suspicion that the two cycles are actually

Table 2
Fossil marine beach chronology for western Morocco.

Formation	Member	Facies	Main sediments	Chronology
Kef El Haroun	Oulad Aj J'mel	Tidal	Shoreface conglomerate and laminated sands, 9–15 m amsl	MIS 9 or 11; OJ1 400 ± 139 ka
		Dune	Aeolianite, cross-bedded bioclastic sands.	OJ2 345 ± 119 ka, OJ2 303 ± 30 ka
	Bir Feghloul	Tidal	Foreshore pebbly bioclastic sands, 7–8 m amsl.	MIS 7?
		Dune	Aeolianite, sandy.	RB1 163 ± 33 ka
Dar Bou Azza	Aïn Roummana	Littoral	Foreshore and backshore bioclastic sands and gravels, 2–6 m amsl.	MIS 5 or specifically 5.5; "Ouljian"
	Lahlalfa	Continental	Red clayey sand slope deposits with floating calcarenite and calcrete clasts.	MIS 2–4; "Soltanian"
Reddad Ben Ali		Littoral	Uncemented gravels and coarse bioclastic sands, 0–3 m amsl.	MIS 1 peak; "Mellahian"
		Dune	Unconsolidated or poorly cemented sands.	ca 4 ka and more recent

both of MIS 5.5 age. The Bir Feghloul Tidal Sub-Member (currently at 7–8 m amsl) should therefore date to 190–198 ka and the Aïn Roummana Littoral Sub-Member (currently at 2–6 m amsl) should date to 118–132 ka; there should be no other 'raised' marine deposits in the vicinity within the timespan of interest here. It may be noted in passing that, in the work of Texier et al. (2002), two out of the four researchers expressed some reservations over correlation between observed marine deposits and main global highstands older than MIS 5.5. That conclusion was probably over-cautious at the younger end of the series (the global background research cited being from the 1980s and 1990s and mostly now superseded) and there would certainly be no reason to doubt that the marine signal from "short return glacio-eustatic events" (Texier et al., 2002, p. 39), such as Heinrich Events or interstadials like MIS 6.5, could be relevant in the present Late-Middle to Upper Pleistocene context.

Turning to the aeolianites (indurated/lithified dune sand), it is rather more difficult to suggest a likely chronological pattern. In the Casablanca area, researchers have either reported explicitly or have implied that dune sands follow the various marine sediments conformably. Indeed, worldwide, it is often found or assumed that there is a strong association between marine highstands (especially during interglacials but also some interstadials) and large-scale dune activity (cf. Brooke, 2001; Brooke et al., 2003). Survival of proximal dunes formed during marine regression is more likely but study of Holocene systems shows that dune activity (original aeolian deposition) is a rather complex function. For instance, Moura et al. (2007) report dune formation during rapid early post-glacial transgression coupled with arid conditions in the Algarve, followed by maximum transgression with a less than critical sand fetch and consequent dune stabilisation and cementation during the damp Atlantic climatic phase, followed by regression with increased sand fetch and renewed dune accumulation, finally halted only as both the sand fetch and sand input by local rivers declined in recent times. McLaren (2007) lists, as factors in coastal dune formation, the prevalence of onshore winds, sediment supply, sea level, ocean currents, continental margin/platform geometry, level of carbonate production, vegetation and climate (precipitation, temperature and potential evaporation). Given this complexity, it is not surprising that many cases of 'non-interglacial' occurrence have been identified. Nielsen et al. (2004) report dominantly cool climate dune fields on Mallorca. Bateman et al. (2004) observed that dunes did not form on the Cape coast of South Africa during interglacials but, rather, during periods of rapid transgression/regression under cooler and wetter conditions (facilitating cementation). Ortiz et al. (2005) found that dunes formed on the Canary Islands at various times during MIS 3–1, whenever there was an abrupt transition from humid to arid conditions associated with shifts in monsoonal wind patterns over Africa. On the coastal plane of Israel (Frechen et al., 2004; Porat et al., 2004), dune formation (and the intervening palaeosol formation) over the last 140 ka does not correlate well with the main glacial–interglacial cycles but does correspond to known local variations in detailed climate and sediment availability affecting the eastern Mediterranean region.

Returning to DeS I itself, the bedrock in which the cave is formed is a very well lithified calcarenite; despite rather poor exposure at outcrop and strong case-hardening with recrystallisation, some large-scale bedding features are still recognisable, so that it may be confirmed that this is a fossil dune (aeolianite) deposit, assumed to be of Pleistocene age. The unit survives only as high as a 'flat' (with small-scale solution irregularities), devoid of any weathering mantle or unconsolidated sediments (probably due to wind deflation), with the cliff exposure in the immediate vicinity usually being only 3–6 m high, before it is masked by talus.

Ruhlmann (1951, Fig. 2) gave a sketch cross-section, from above the cave, across the dune slack, over the consolidated seaward dune and down to the sea, with heights expressed in metres 'above sea level'. An accurate geodesic datum is not currently available in the immediate vicinity. We have noted that Ruhlmann's heights appear to show constant over-estimation with respect to GPS estimates (both with and without barometric correction). We have therefore taken the primary marine planation bench (or, more exactly, the surface of the retained water basin exposed during low tide but well covered during high tide, at 33°58′51.6″N, 6°53′54.8″W) as a reasonable surrogate (within about 1 m accuracy) for mean sea level, a datum which we label here as '≅msl'. On this basis, we have surveyed (by total station) the rock surface immediately above the entrance to DeS I at 13.52 m a≅msl.

Within the cave, sediment Groups 2–5 are wholly terrestrial (see below) but the lower part of Group 1, despite its currently very restricted exposure, can be firmly identified as an *in situ* 'raised beach' deposit. The clear bedding forms (including lenses of marine shell), textural and compositional grading characteristics and intraformational deformation structures indicate that this is an upper shoreface facies, deposited at constant, relatively low energy (that is, not in a major surf zone) over a significant period of time; there is no possibility that this material is the 'instantaneous' result of a tsunami or storm surge event. Ruhlmann noted 0.35 m of shelly beach sand (Layer M) but believed that, below this, he had found the 'floor' of the cave at ca 9 m 'above sea level'; our field observations show that he had only reached a better cemented zone within these sands, which have still not been bottomed, although more than 1 m thickness of well bedded material has now been proven. We have surveyed the top of unit G1.4 at 4.07 m a≅msl.

The upper part of Group 1 comprises an interval of recrystallised, somewhat shelly coarser sand (the partially turbated top of the beach, Ruhlmann's Layer L), followed by a series of planar, often laminated, beds (dominated by fine to medium sand but with clay loam and carbonate lenses, usually altered and replaced by manganese-rich 'wad', Ruhlmann's Layer K) dipping consistently and quite strongly westwards out of the cave. Although this sequence obviously represents a shift from a dominantly marine source to terrestrial conditions, it is noteworthy that the surviving traces of bedding within the coarser sand, after a basal unit of possible 'beach rock' (material cemented

subaerially but within the reach of salt spray), gradually take on the dip of the overlying laminated terrestrial beds, with no obvious hiatus. Most of the sediments of Group 1 appear to have accumulated quite quickly and it seems likely that the overall Group 1 chronozone, at least as currently exposed, was relatively short, probably less than 10 ka. However, the whole of Group I is indeed truncated by a strong angular unconformity (usually associated with welding by carbonate cement) dipping in an irregular manner back into the cave.

No contact has yet been observed between any level of Group 1 and the bedrock; indeed, the base of the aeolianite unit, whether lying upon earlier Pleistocene beds or upon a pre-Quaternary basement, has not been exposed in the vicinity. There is therefore a *theoretical* possibility that Group 1 actually pre-dates (underlies) the aeolianite, the pair forming a 'normal' (open-air) regressive sequence of the type recognised regionally along this coast, the apparent association with a (later) cave being misleading. However, the extreme difference in degree of lithification between the aeolianite and the various Group 1 units would then be unexplained and unprecedented in any of the exposures reported in the Casablanca area. This hypothesis is therefore rejected in favour of the much simpler explanation that Group 1 is a largely exogenic part of the fill of a cave formed within the (older) aeolianite. The capping unconformity represents a time gap of unknown duration, although the phenomena observed would suggest significant geomorphological changes, probably a sequence of events involving a drop in sea level and the subsequent (re)development of lower karst cavities followed by groundwater and/sea level fluctuation/rise, creating instability and sediment subsidence at a location within the cave not yet exposed. Indeed, we have identified a new karst cavity (Kehf Ayrod, at 33°58′43.8″N, 6°53′51.9″W), which intersects with the exterior slope below the entrance to DeS I at 3.95 m a≅msl and extends down (before its current fill surface) to 0.10 m a≅msl; such low-level caves could not form or be fully sedimentologically active during a period of high sea level, such as MIS 1 or 5.5.

Ruhlmann believed that the DeS I cave was actually formed by the same high sea level which more or less immediately began to deposit the beach sands. There is no evidence to support this hypothesis. Had the sea, necessarily acting along a broad front, been the primary speleogenetic agent, one would have expected a very much more accidented cliff line, with many such features, not to mention distinctive smaller-scale morphology (phytokarstification, halokarstification). Rather, the cave was probably formed, to a length of at least 40 m, along a preferential weakness (a fault line in the aeolianite, perhaps) by normal endogenetic processes, although development may well have been dominantly vadose, with no significant early phreatic stage. Whether or not the marine phase was sufficient to empty the cave of all earlier deposits, or to have notched the bedrock locally, remains to be seen.

The main geological events which constrain the chronostratigraphy of the site are therefore as follows.

First, a body of carbonate-rich sand dunes was formed. This material was then lithified to form aeolianite. Dune sand is often affected by water passing along bedding planes, rather than vertically, thus facilitating mass cementation (cf. McLaren, 2007). Case-hardening or even lithification of thicker but still superficial zones can sometimes be extremely rapid under conditions favouring very rapid oscillation across the aggressive/supersaturated boundary, most commonly observed in the salt spray zone of beaches. Surface hardening can also be caused by vegetation, which itself can help to trap extra sand. Moderate rates of lithification may arise under generally warm climate with oscillating rainfall and evaporation, and especially towards the dune base, near the watertable or a low-permeability subsurface. If favourable conditions are not present, calcareous dunes may remain unlithified for millennia or even tens of millennia. In the present case, it is therefore difficult to estimate, from sedimentological principles, the minimum time needed to produce a competent aeolianite at DeS I, from deposition to lithification. Future micromorphological study of the cement would help by showing the dominant process(es) of diagenesis (cf. Graoui in Texier et al., 2002; McLaren, 2007). For the present, it would seem reasonable to suggest a span of about 10 ka, with shorter timescales appearing increasingly less likely.

In theory, karstification, at least micro-karstification, could start before full lithification. However, a long and wide cavity could not develop until the substrate was strong enough. Vadose cave formation is another process of uncertain timescale, especially since aeolianite does not lend itself to long systems with phased morphological and speleothem development, attributes which are essential for genetic study. Nevertheless, an estimate of another 10 ka seems a reasonable minimum.

Now, if Group 1 was deposited in MIS 5.5, the aeolianite bedrock could date from any dune phase prior to about 150 ka (allowing a minimum time for lithification and karstification); the remaining cave sediments, above the major unconformity, would post-date MIS 5.5. If, however, Group 1 was to date from MIS 7.1, the aeolianite would be unlikely to be an intra-MIS 7 phenomenon (because of the relatively constantly high sea levels and the consequent threat to the stability of the dune), more likely deriving from some period prior to 260 ka. The date of the cave sediments above the major unconformity would not be so constrained; they might still contain only 'post-Last-Interglacial' material (long time gap) or they might include some older deposits, including a non-marine representative of the Aïn Roummana Littoral Sub-Member interval. It was assumed by Ruhlmann, and in all the succeeding literature, that the Group 1 high stand was of "Ouljian" (approximately MIS 5.5) date; this would constrain the overlying sediments to be 'post-last-interglacial' and thus broadly valid as a type sequence for the "Soltanian", as envisaged by Choubert et al. (1956), although the presence of the major unconformity requires recognition that there is some gap in the sequence. The altitude (3–4 m a≅msl) at which the DeS I beach deposits are observed is significantly dissimilar to (lower than) that of the open-air Bir Feghloul Tidal Sub-Member (MIS 7) in the Casablanca area, a factor which would now appear decisive.

The upper part of the Bir Feghloul Member is a thick dune sand dating broadly from MIS 6. Whilst there is no aeolianite body formally included in the definition of the later part of the Dar Bou Azza Formation, aeolian sands do occur in a post-MIS 5.5 context at various points in the Casablanca area. At Dar es-Soltan, there is a low ridge of aeolianite (today reaching a height of ca 10.8 m a≅msl at the crest) seaward of the cave; an outer notch in this lithified dune, to ca 1–2 m a≅msl, is probably referable to the earlier Holocene (Mellahian).

The slack between the two dune lines holds a variable thickness of red loams (which contain Neolithic, Upper and Middle Palaeolithic artefacts in correct superposition, suggesting undisturbed open-air stratigraphy) above extremely weathered aeolianite; it is not currently clear whether the two dunes were already present in MIS 5.5 (implying a lagoonal shore below DeS I) or whether the seaward dune developed later. The significant point here is that, if the seaward dune post-dated MIS 5.5, the area around the cave may well have been denuded of significant thicknesses of aeolian sand before cementation could provide sufficient resistance to erosion; the very presence of the outer dune-form would necessarily increase deflation immediately inland. The cave mouth must have been open during the deposition of Group 1 but the whole area could have been buried under a thick dune during the period represented by the major unconformity cutting Group 1. The cave mouth was open again during the deposition of Group 2, since

there is a continual archaeological presence, but there could still have been a relatively thick cover above the cave. Only in Group 3 is there clear evidence of sediment input via the (forward) opening in the roof, implying that there was no longer a thick mantle of unconsolidated material at the surface above.

The detailed lithogenesis of Groups 2–5 will be the subject of future study. Anthropogenic effects are very strong in Group 5 (sometimes obscuring other mechanisms), strong in Group 3 (with repeated hearth events), a little less so in Group 2 but not obviously significant in Group 4 (despite the presence of archaeological material). Groups 2–3 comprise very well structured units, often laminated, with sandy, silty and even clayey loam segregation at times but relatively poorly sorted in bulk. There are common cemented lenses, derived 'eucladiolith' accumulations (calcareous phytotufa clasts, fallen from their growth positions on cave walls and ceiling) and even some minor travertine lenses, stalagmitic bosses and other small-scale speleothem forms. There is widespread bioturbation (especially in Group 3, where human treadage may also be a factor) and alteration ('rotting') of bedrock clasts. Ichnofossils (trace fossils) clearly include many intraformational examples, probably due mostly to burrowing in-fauna (insects and mollusca for the smaller forms, rodents and reptiles for the larger forms) but with some dendritic forms referable to rooting (there has been recent plant root penetration and further study will be needed to demonstrate more accurately the stratigraphic origins of ancient forms). All these characteristics suggest moist (at least seasonally), biologically active environments more or less throughout the Groups 2–3 interval, with occasional really wet events (producing significant sheet erosion), contrasting strongly with the modern, relatively arid conditions. The Group 4 sediments still show some carbonate concretions. The bed-forms are quite subtle but include continual reactivation of troughs at various scales, indicating aggressive water-erosion. The finer sediments are dominated by silts and fine sand, giving slightly better bulk sorting (and much better sorting within certain individual lenses and laminae) than in the underlying Groups, suggesting more common secondary (wash) derivation from wind-blown source materials. Ichnofossils are usually small-scale and much less densely spaced than in underlying beds. Bedrock clasts are generally more common, even ignoring the larger (boulder) elements, for which any palaeoenvironmental signal will be strongly masked by historical structural factors. Overall, the Group 4 sediments seem to suggest relatively unstable mechanical conditions (strong fluctuations in effective humidity), with lower levels of biological and chemical activity. The lower part of Group 5 is a loamy fine sand, again suggesting wash deposition probably including an ultimately aeolian source; post-depositional bulk turbation (perhaps including human action) is obvious in some places but there are also zones of better stratified material.

4. Re-assessment of the Aterian assemblages

Most of the Ruhlmann lithic artefact collection from DeS I is still preserved in the Archaeological Museum in Rabat. Each of the three recognised assemblages is briefly reviewed in turn.

The Aterian from the lowermost layer (I) can be confirmed to be predominantly of flints and other fine-grained siliceous rocks with relatively small quantities of quartzite. The lithic technology displays a significant Levallois component including triangular flakes and small cores. However, we have noted that amongst the small cores that only two are typical Levallois examples, while the rest (12) are discoidal forms (Fig. 3). The collection is rich in simple points that could have been produced from small cores though some of them clearly originated from larger cortical flakes (e.g. Ruhlmann, 1951, Fig. 18, no. 5). Interestingly, the Levallois technique is more commonly present on fine-grained siliceous rocks and

Fig. 3. Dar es-Soltan I. Small Levallois and discoidal cores. Top row: examples from Ruhlmann's Aterian assemblage I; bottom rows: examples from Ruhlmann's Aterian assemblage C2.

Fig. 4. Retouched tools from Ruhlmann's Aterian assemblage I. Left to right. pedunculate point (quartzite), convergent side scraper, bifacially flaked foliate point, retouched blade (quartzite), pedunculate point.

rarely on quartzite. From raw material studies (Bouzouggar, 1997a), it appears that large cobbles of quartzite are locally available in the Rabat–Témara area near the rivers Yquem and Bouregreg, as well as in some marine terraces. This can be contrasted to the flint which is found east of Rabat but also occurs in the form of small pebbles near the Yquem river, about 20 km from DeS I.

Amongst the retouched tools are side scrapers, end scrapers and denticulates. The most characteristic implements can be defined as pedunculates of which 25 examples are preserved in the Museum collection today (Fig. 4). The blanks are basically Levallois products but some pedunculates were made on non-Levallois flakes and partially cortical pieces. The tangs generally occupy up to a third of the total length of the tool and are most often developed on the proximal ends of elongate flake blanks with some still retaining the original bulb of percussion. Where retouch occurs on the main body of the tool it is usually flat and invasive and restricted to the dorsal surface. Occasionally retouch is also visible on ventral surface of the tang itself (Ruhlmann, 1951, Fig. 20). Unlike Ruhlmann we were able to recognise two bifacial foliates in this assemblage (Fig. 4). Both are on laminar flakes and are made on thin clasts of silicified limestone. Such blade-like flakes are relatively common in the industry of Layer I and may reflect an opposed platform technique and the use of soft stone hammer percussion. The two ivory objects, one shaped like a point and the other a small *plaquette*, are currently under study.

The lithic artefacts in the overlying (C2) reflect the use of Levallois and discoidal core technology similar to that described in I (Fig. 3). Elongate and laminar flakes are quite common though few

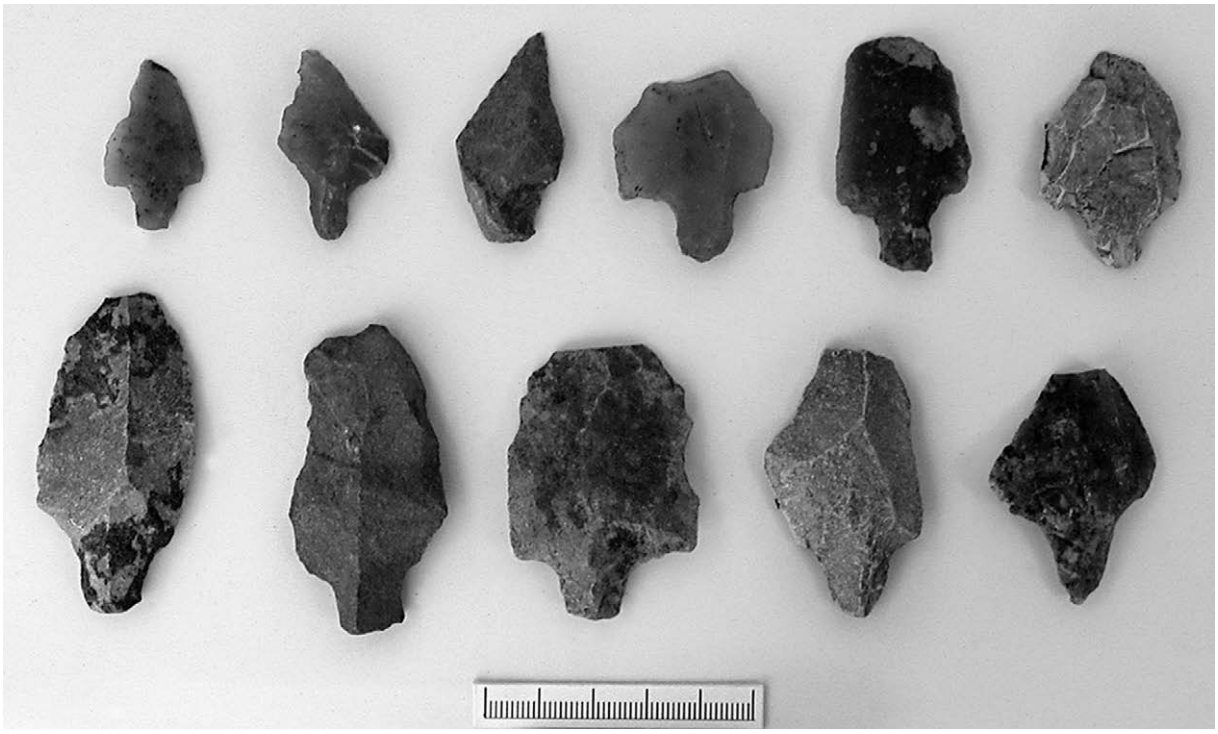

Fig. 5. Retouched tools from Ruhlmann's Aterian assemblage C2. Top row, left to right: Pedunculate points.

can be described as true blades. The raw material is dominated by flint, with some of the larger flakes being made of quartzite that probably originated from gravels of the Yquem river.

The range of retouched tools represented is very similar to that of the lower industry. The inventory includes a variety of side scrapers, mostly offset examples (*racloirs déjetés*) and made of flint, more rarely of quartzite. Although burins were recorded by both Ruhlmann (1951) and Roche (1956), re-examination shows that these are accidental *Siret* breaks (Bordes, 1961). The pedunculates (21) are generally made on elongate blanks and especially Levallois products (Fig. 5). In contrast to the industry in I, they occur on a noticeably wider range of tool types. They include points, such as the eponymous *pointe marocaine* (Ruhlmann, 1951, Figs. 33, no. 8), a narrow and bifacially flaked tanged point that resembles a projectile type. Apart from this example, other pedunculates are on thicker blanks and some have been modified into scrapers so we would not ascribe a specific function to these tanged tools. Indeed our preliminary use-wear studies on Aterian points from sites in north-eastern Morocco show that they were used in a variety of ways for cutting and other processing tasks (Bouzouggar et al., 2007b).

Re-assessment of the third assemblage, from C1, is complicated by the fact that some of the artefacts were discovered near the entrance while others came from inside the cave (Ruhlmann, 1951, p. 59) and it is now difficult to distinguish between them in the present collection. Our analysis has confirmed that the most common raw materials are again locally sourced flints and quartzites. The technology features small discoidal cores and there is a focus on flake production (Fig. 6). Many of the flake butts are plain or cortical and there are few prepared examples. Interestingly, in contrast to the lower archaeological assemblages the quartzite flakes include many more cortical specimens implying that quartzite was brought to the site as cobbles and knapped *in situ*. Amongst the cores is a small bladelet core which could be intrusive from Layer B (our unit G5). However, similar finds have previously been noted in Aterian contexts at Contrebandiers (Roche, 1963, 1976; Bouzouggar, 1997b) as well as bladelets in eastern Morocco (Wengler, 1993) and it is likely that the core from C1 is genuinely from the Aterian. Amongst the very small collection of retouched tools are side scrapers, an atypical Mousterian point and a bifacially flaked rectangular form. There are no pedunculate tools in this assemblage.

In addition to the finds referred to above, during our work at the site in 2005 we discovered two pedunculate points in the main section of the site, one in our G2 sequence (equivalent of Ruhlmann's F–J which includes Layer I) and one in G3 (equivalent of Ruhlmann's D–E series). Indeed it is clear from our preliminary fieldwork that many more archaeological horizons are identifiable than originally understood by Ruhlmann.

5. OSL dating methodology and new results

Optically Stimulated Luminescence (OSL) dating provides an estimate of the time elapsed since luminescent minerals, such as quartz or feldspar, were last exposed to sunlight (Huntley et al., 1985; Aitken, 1998). Light-shielded grains may accumulate charge from the effects of the environmental radiation flux to which they are exposed and the dose received by the sample, also referred to as the palaeodose, can be measured using the luminescence signal. A burial age estimate is obtained by dividing the palaeodose by the environmental dose rate. OSL dating of sedimentary quartz has become a well established technique within Quaternary science (Duller, 2004; Lian and Roberts, 2006) and recent applications to archaeological sites in Australia (Prideaux et al., 2007), Morocco (Bouzouggar et al., 2007a; Mercier et al., 2007), Spain (Berger et al., 2008) and South Africa (Jacobs et al., 2003a,b, 2006, 2008b) demonstrate the high potential of optical dating for securing chronological frameworks in caves and rock shelters.

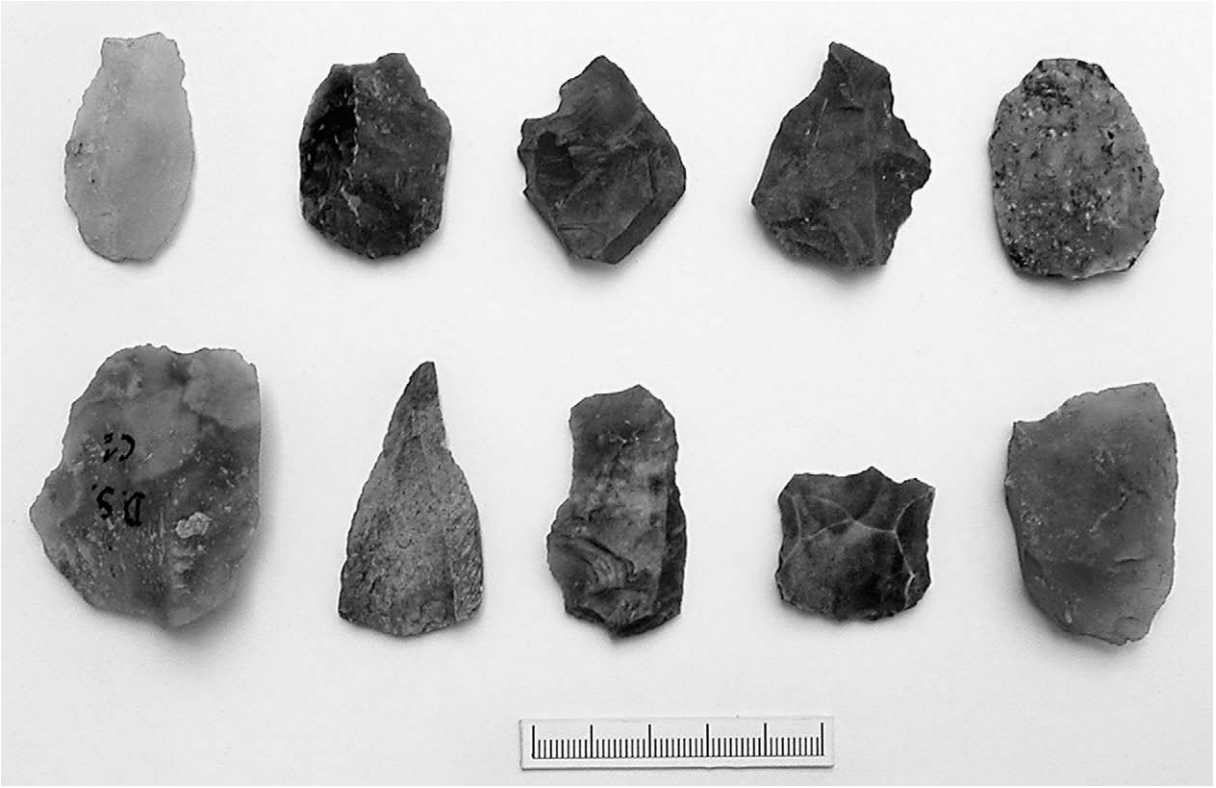

Fig. 6. Flakes from Ruhlmann's assemblage in C1. Top row: Levallois and discoidal flakes; bottom row: Levallois point (2nd from left), side scrapers (4th and 5th from left).

5.1. Methodology

Luminescence dating was based on quartz grains extracted from a series of twenty two samples (Fig. 2) collected in June 2005 from the exposed longitudinal section left by Ruhlmann. All sample preparations took place under low intensity safe-lighting provided by filtered sodium lamps (emitting at 588 nm) at the Luminescence Dating Laboratory of the Research Laboratory for Archaeology and the History of Art, University of Oxford. Laboratory procedures were designed to yield sand-sized (180–250 μm) grains of quartz for optical dating according to standard preparation methods, including wet sieving, HCl acid digestion, density separation and etching in 68% HF acid to dissolve feldspar minerals and remove the outer 6–8 μm alpha-dosed layer. OSL measurements were conducted using an automated system (Risø TL/OSL-DA-15 reader) and are based on a conventional single-aliquot regeneration (SAR) measurement protocol (Murray and Wintle, 2000). Palaeodose estimates were obtained for small sized aliquots (~2 mm diameter) comprising ca 50–100 grains and 6–18 repeat measurements were made for each sample. Optical stimulation for single aliquots was provided by blue light emitting diodes (42 Nichia 470Δ20 nm; 36 mW cm^{-2}) and initial complementary single-grain studies were carried out using a focused green laser beam (Nd:YV04 diode pumped laser; 532 nm; 10 mW). The natural and regenerative doses were preheated at 260 °C for 10 s, and the fixed test doses (which are used to correct for any sensitivity changes) were preheated at a reduced temperature of 240 °C for 10 s, before optical stimulation. The absence of infrared-sensitive minerals (e.g., feldspars) was checked and confirmed using an infrared bleach provided by a solid state laser diode (830Δ10 nm; 1 W cm^2) at 50 °C for 100 s before blue or green-light stimulation. The ultraviolet OSL emission at ~370 nm was detected using an Electron Tubes Ltd 9235QA photomultiplier tube fitted with a blue-green sensitive bialkali photocathode and 7.5 mm of Hoya U-340 glass filter. Laboratory doses used for constructing dose–response curves were given using a calibrated $^{90}Sr/^{90}Y$ beta source housed within the reader. Some typical example OSL data pertaining to samples OSL 9 and OSL 5b are plotted in Figs. 7 and 8.

To calculate dose rates, we combined the results of *in situ* γ-ray spectroscopy measurements with elemental analysis by inductively coupled plasma mass spectroscopy (ICP-MS) using a lithium metaborate/tetraborate fusion carried out by Actlabs (Canada). A portable gamma-ray spectrometer (Ortec Micronomad multi channel analyser equipped with a 3 × 3 inch NaI (Tl) scintillator crystal) was employed in a 4 π-geometry and calibrated against the Oxford calibration blocks (Rhodes and Schwenninger, 2007). These on site measurements provided direct estimation of the total *in situ* gamma radiation field (~30 cm radius sphere of the sampling location). The beta dose rate was derived from the concentrations of potassium, thorium and uranium obtained by the laboratory-based elemental analyses of sub-samples of sediment. The cosmic-ray dose was calculated according to standard data reported by Prescott and Hutton (1994), taking into account the height of the overburden, including the thickness of the cave roof, as well as the geomagnetic position of the site (latitude, longitude and altitude). Estimates of radionuclide concentrations were converted to dose rates according to attenuation factors proposed by Adamiec and Aitken (1998), using corrections for grain size (Mejdahl, 1979) and water content (Zimmerman, 1971). The past water content of the sediments may at times have deviated from the modern field values but none of the samples were located near a drip line nor are they believed to have been fully saturated for prolonged periods of time. The present moisture contents may therefore be considered to represent the best approximation of the average water content of the samples throughout their burial history. To accommodate any significant attenuation effects caused by past changes in pore water on the total dose rate received by the quartz mineral grains, relatively large systematic errors were attached to individual values (see Table 3).

5.2. OSL results

Multi-grain palaeodoses were determined from the first 2 s of OSL, using the final 10 s as background noise whereas for single-grain measurements, palaeodoses were obtained from the first 0.25 s of the natural and regenerated OSL signals, using the final 0.10 s as background counts. Dose–response curves (Fig. 8) were fitted using a saturating-exponential-plus-linear function, with the standard error on the palaeodose determined by Monte Carlo simulation (1000 iterations) or using a weighted linear fitting procedure based on propagation of all measurement errors. A systematic laboratory reproducibility uncertainty of two percent was added (in quadrature) to each OSL measurement error to account for uncertainties in the calibration of the beta source.

Dose recovery measurements were obtained for three aliquots of four randomly chosen but evenly spaced samples (OSL 1, OSL 5b, OSL 12 and OSL 16) spanning the entire stratigraphic sequence.

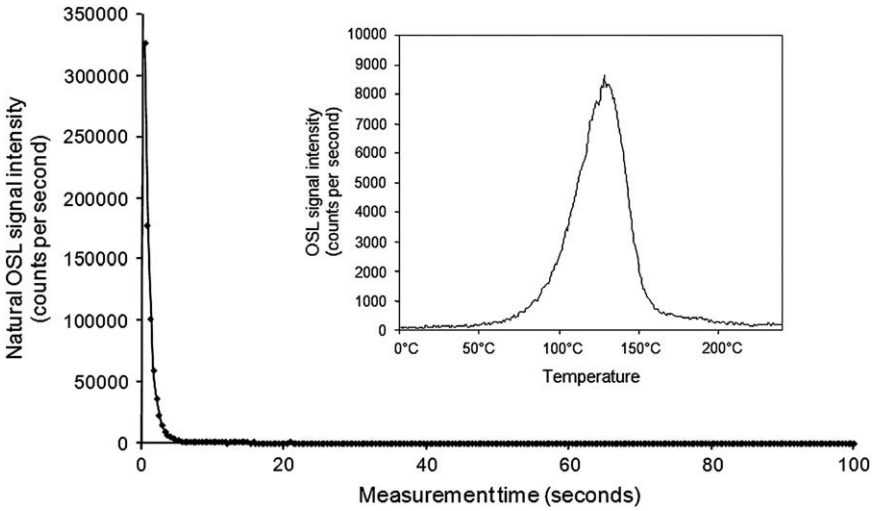

Fig. 7. Typical natural OSL signal (black line with diamond markers) recorded from a small (1–2 mm) multi-grain aliquot of sample X2385. The insert figure (thin black line) shows the preheat response of the same aliquot following a small test dose.

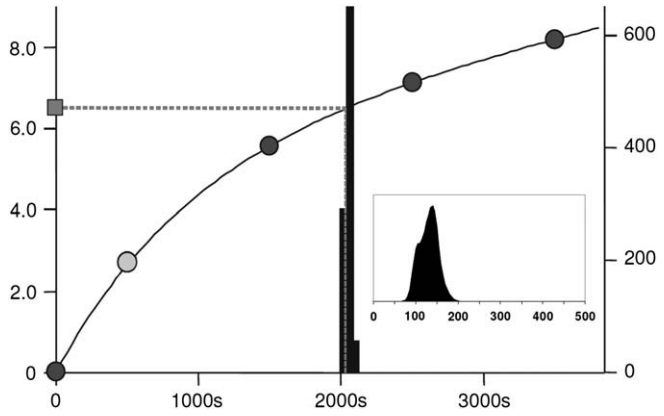

Fig. 8. Typical SAR dose–response curve for a multi-grain aliquot from sample X2381. The grey square on the left *Y* axis (sensitivity corrected OSL in counts per second) represents the natural OSL signal. The dark grey circles are the regeneration dose points and the light grey circle marks the repeat dose point which fits perfectly with the first regeneration point. The interpolated palaeodose is based on Monte Carlo repeats (right *Y* axis; frequency of repeats) and is equivalent to ca 100 Gy (*X* axis; irradiation time in seconds). The small insert plot shows the probability distribution of six palaeodose values which provide a mean weighted value of 126.33 ± 8.94 Gy using a central age model.

These had been bleached in daylight for 100 s prior to any measurements and then given a known laboratory dose equivalent to 69.12 Gy. Under the experimental and analytical conditions outlined above, correct dose estimates were obtained in all cases, providing a mean ratio of measured/given doses of 1.01. Interestingly, the same test conducted on grains bleached for the same amount of time by blue LED illumination (95% power) inside the luminescence reader systematically resulted in slightly reduced, although acceptable recovered doses characterized by a mean ratio of 0.96. One of the aliquots from sample OSL 1 used in the dose recovery experiment produced a clear infrared signal indicating the presence of at least one contaminant feldspar grain. However, the recovered dose remained within 8% of the administered dose thus demonstrating the robustness of the adopted post-IR blue measurement protocol. The dose recovered from the IR signal produced a more satisfactory ratio of 0.96.

Otherwise, very few aliquots showed signs of feldspar contamination (see Table 4) suggesting high sample purity and confirming good sample preparation and/or relative sparseness of feldspathic components amongst the mineral components of the cave sediments. A one percent limit on the initial count ratio of IRSL/OSL was used as a rejection criterion and only one aliquot of sample OSL 15 and eight aliquots from OSL 21 failed this test. The latter, was collected from the presumed aeolianite substrate in which the cave is formed. The quartz mineral grains within the parent bedrock may have a different origin (reworked marine sediments) compared with the loose infill of the cave. The latter is considered to originate largely from eroded soil material and terrestrial sediments which have been washed in through large holes in the roof of the cave. Subsequent alteration of the sediments including their exposure to heat and the admixture of additional material through human and animal presence is also likely to have occurred. Differences in the behaviour and the characteristics of the observed luminescence signal may thus reflect differences in the origin of the source material as well as being indicative of post-depositional alterations to the physical and chemical properties of the sediment through anthropogenic activity. Such effects are currently being investigated as part of a wider research initiative into the study of Aterian cave sites in Morocco and which will include more detailed single-grain analyses of these samples.

Results from the multi-grain single aliquots studied here displayed very high sensitivity with initial signal intensities often in excess of 100,000 counts per second and the OSL shine down

Table 3
Dose rates, palaeodose values and calculated OSL age estimates for the Dar es-Soltan I samples. Radionuclide concentrations and dose rates highlighted in italics are considered to be problematic because of the highly altered nature of the corresponding cave sediment and age estimates obtained for these samples may be unreliable.

Sample field code	Sample laboratory code	Radioisotopes[a]			Field water (%)	External γ-dose rate[c] (Gy/ka)	Total dose rate (Gy/ka)	Palaeodose (Gy)	Age (ka)
		K (%)	Th (ppm)	U (ppm)					
OSL 1	X2376	*0.07*	0.5	1.1	2–8	0.244 ± 0.012	0.49 ± 0.02	74.08 ± 3.20	151.4 ± 9.1
OSL 2	X2377	0.36	2.2	1.4	9–19	0.294 ± 0.015	0.76 ± 0.04	84.73 ± 4.25	112.1 ± 8.1
OSL 3	X2378	0.45	2.7	1.0	16–26	0.315 ± 0.031	0.76 ± 0.04	86.38 ± 5.00	113.9 ± 9.7
OSL 4	X2379	*0.34*	*2.5*	*1.2*	19–29	*0.335 ± 0.017*	*0.72 ± 0.03*	113.82 ± 7.51	157.5 ± 12.8
OSL 5A[b]	X2380	0.60	4.3	1.5	11–21	0.433 ± 0.022	1.08 ± 0.05	115.23 ± 4.93	107.1 ± 7.3
OSL 5B[b]	X2381	0.66	5.4	1.7	11–21	0.433 ± 0.022	1.15 ± 0.06	126.33 ± 8.94	109.9 ± 9.8
OSL 6	X2382	0.63	3.5	1.9	13–23	0.513 ± 0.026	1.18 ± 0.06	145.65 ± 7.84	122.9 ± 9.1
OSL 7	X2383	0.51	4.7	1.6	14–24	0.401 ± 0.020	0.99 ± 0.05	110.67 ± 8.24	111.9 ± 10.1
OSL 8	X2384	1.45	4.0	1.7	9–19	0.692 ± 0.035	1.88 ± 0.11	147.62 ± 6.07	78.4 ± 5.7
OSL 9	X2385	1.25	3.9	1.9	15–25	0.638 ± 0.032	1.65 ± 0.09	147.50 ± 6.26	89.5 ± 6.4
OSL 10	X2386	1.44	4.1	1.9	10–20	0.676 ± 0.034	1.87 ± 0.11	166.28 ± 4.69	88.7 ± 5.9
OSL 11	X2387	1.45	4.7	2.1	10–20	0.686 ± 0.034	1.92 ± 0.11	140.01 ± 7.88	72.8 ± 6.0
OSL 12	X2388	1.16	4.3	1.7	12–22	0.552 ± 0.028	1.55 ± 0.09	95.44 ± 3.97	61.7 ± 4.4
OSL 13	X2389	1.02	4.8	1.8	9–19	0.548 ± 0.027	1.53 ± 0.08	80.51 ± 1.56	52.8 ± 3.2
OSL 14	X2390	0.71	3.6	1.6	3–9	0.499 ± 0.025	1.33 ± 0.06	43.99 ± 2.32	33.0 ± 2.3
OSL 15	X2391	0.57	3.5	1.4	2–8	0.444 ± 0.022	1.17 ± 0.05	8.98 ± 0.45	7.6 ± 0.5
OSL 16	X2392	0.38	2.3	1.0	9–19	0.212 ± 0.011	0.71 ± 0.03	4.82 ± 0.10	6.8 ± 0.4
OSL 17	X2393	0.20	1.3	1.3	9–19	0.200 ± 0.010	0.54 ± 0.02	70.35 ± 8.80	131.4 ± 17.7
OSL 18	X2394	1.23	3.8	1.4	9–19	0.645 ± 0.032	1.68 ± 0.09	113.47 ± 5.90	67.7 ± 5.3
OSL 19	X2395	*1.28*	*1.7*	*7.4*	16–26	*0.749 ± 0.037*	*2.24 ± 0.12*	348.34 ± 24.76	155.5 ± 14.2
OSL 20	X2396	0.35	2.6	0.8	31–41	0.300 ± 0.015	0.60 ± 0.02	84.39 ± 5.04	139.8 ± 10.5
OSL 21	X2397	0.23	0.7	1.9	0–6	0.345 ± 0.050	0.93 ± 0.07	193.79 ± 23.30	209.2 ± 29.5

[a] Measurements were made on dried, homogenised and powdered material by ICP-MS with an assigned systematic uncertainty of ±5%. Dry beta dose rates calculated from these activities were adjusted for the measured field water content expressed as a percentage of the dry mass of the sample.

[b] Samples OSL 5a and OSL 5b are near replicates taken from the same stratigraphic unit and located within 15 cm horizontal distance of each other. γ-ray spectroscopy measurements were made at the location of OSL 5b and the same external gamma dose rate was applied to sample OSL 5a.

[c] Based on *in situ* measurements using a portable γ-ray spectrometer equipped with a 3 × 3 inch NaI (Tl) scintillator crystal and calibrated against the Oxford calibration blocks (Rhodes and Schwenninger, 2007). No field spectroscopy measurements are available for samples OSL 3 and OSL 20. For these, we used values based on the mean external γ-dose rate of directly underlying and overlying samples. In the case of OSL 21, measurements were obtained from a natural hole located in the aeolianite bedrock.

Table 4
Quality control criteria and test results relating to single-aliquot regenerative-dose OSL measurements of samples from Dar es-Soltan I.

Field code	Laboratory code	Aliquots rejected (%)	Mean IRSL (% of OSL[a])	Mean recycling ratio	Mean thermal transfer (%)
SOL105-01	X2376	0	0.18	0.979 ± 0.019	0.006 ± 0.001
SOL105-02	X2377	0	0.12	1.008 ± 0.020	0.006 ± 0.001
SOL105-03	X2378	0	0.04	1.012 ± 0.005	0.008 ± 0.001
SOL105-04	X2379	0	0.08	N/A	0.006 ± 0.002
SOL105-05A	X2380	0	0.10	0.979 ± 0.006	0.017 ± 0.001
SOL105-05B	X2381	0	0.18	0.998 ± 0.005	0.005 ± 0.001
SOL105-06	X2382	0	0.07	0.996 ± 0.006	0.011 ± 0.001
SOL105-07	X2383	0	0.18	0.984 ± 0.004	0.006 ± 0.001
SOL105-08	X2384	0	0.05	0.959 ± 0.005	0.020 ± 0.001
SOL105-09	X2385	15	0.03	0.951 ± 0.007	0.019 ± 0.002
SOL105-10	X2386	25	0.04	1.011 ± 0.017	0.010 ± 0.001
SOL105-11	X2387	0	0.01	0.994 ± 0.014	0.005 ± 0.000
SOL105-12	X2388	0	0.05	0.997 ± 0.011	0.007 ± 0.000
SOL105-13	X2389	15	0.02	1.058 ± 0.008	0.008 ± 0.000
SOL105-14	X2390	0	0.20	1.004 ± 0.008	0.007 ± 0.001
SOL105-15	X2391	15	0.25	1.020 ± 0.003	0.022 ± 0.004
SOL105-16	X2392	0	0.16	1.006 ± 0.009	0.016 ± 0.002
SOL105-17	X2393	0	0.10	1.014 ± 0.007	0.009 ± 0.002
SOL105-18	X2394	15	0.02	0.980 ± 0.005	0.008 ± 0.001
SOL105-19	X2395	0	0.10	0.977 ± 0.005	0.008 ± 0.101
SOL105-20	X2396	10	0.11	0.875 ± 0.023	0.164 ± 0.026
SOL105-21	X2397	60	0.57	0.992 ± 0.016	0.012 ± 0.002

[a] Derived from 1st channel counts of the natural signal.

curves typically display a strong and fast decreasing signal (Fig. 7). Complementary initial single-grain measurements further demonstrated the prevalence of bright grains with an average of 60% of all the grains providing a detectable OSL signal. Most samples also provided a well defined 110 °C TL peak (see insert Fig. 7) which is characteristic of quartz. Routine repeat measurements of the luminescence signal resulting from the first regeneration dose (recycling test) indicate that the adopted SAR procedure is providing adequate correction for changes in the sensitivity. Except for sample OSL 20, most samples are characterized by excellent recycling ratios (see Table 4) with mean values typically in the range of 0.97–1.02. The same is also true for recuperation (Aitken and Smith, 1988) which is generally below 0.1% as monitored by the OSL response after a regeneration dose of zero. This index falls well below the 5% mark suggested for the SAR thermal transfer test proposed by Murray and Wintle (2000).

The measured SAR palaeodose values and the calculated OSL age estimates are shown in Table 3. With the exception of sample OSL 19, which was deliberately collected from the weathered outer rim of a large boulder fallen from the roof of the cave, the dates are considered to be reliable and are in good stratigraphic order, thus providing additional reassurance that mineral grains were bleached before deposition. The latter sample has a suspiciously high uranium content of 7.4 ppm compared to the other samples in the series. This could be related to post-depositional uptake of uranium following chemical weathering processes around the edges of the boulder. The inflated high dose rate could provide a serious age underestimate and for this reason, this OSL date should be considered to be unreliable.

In order to obtain an improved resolution on the chronology of the cave deposits and given the relatively high number of samples and their clear stratigraphic relationships, we used the freeware Oxcal software package (version Oxcalv4.1b2) written by Christopher Ramsay (University of Oxford) to create a Bayesian model (Bronk Ramsey, 1995, 2001; Rhodes et al., 2003) for the long term sedimentary sequence represented at DeS I. The model imposes a simple sequential order upon the calculated OSL age estimates based on depth measurements and secure stratigraphic relationships between the samples. Each date corresponds to a separate dated event, except for the pair of replicate samples OSL 5a and OSL 5b which were entered as sub-samples of the same event. Following Rhodes et al. (2003), systematic errors (in this case, the water content error) were removed from the dates before they were entered into the model and then reincorporated after the run.

The output of the Bayesian analysis is graphically represented as an age–depth model in Fig. 9 and the tabulated results with a resolution of 200 years are shown as an insert. The modelled OSL age estimates provide a good chronological framework for the site even though the dates obtained for some of the basal samples remain less well constrained. In contrast to the more homogenous fine textured nature of most of the cave infill, these coarse lower sedimentary units are largely dominated by comminuted marine shell fragments. We suspect that the presence of large carbonate particles and associated large pore spaces as well as localized cementation and microscale variations in pore water may considerably complicate the correct evaluation of the dose received by individual quartz grains lodged within the sedimentary matrix. The enhanced degree of scatter observed among individual measurements on single multi-grain aliquots from samples within the lower Group 1 was also confirmed by some of our initial single-grain measurements. It is possible that the problem may be related to the incorporation of grains with a residual geological signal. Given the high energy depositional context of these marine sands, this would not come as a surprise. However, it is worth pointing out that the age estimate obtained for the sample collected from the aeolianite bedrock (OSL 21) suggests a relatively young age of ca 210 ka for this geological formation. Consequently, any grains derived through the disaggregation and reworking of minerals originating from the oldest geological material available in the surroundings of the cave are not expected to completely falsify the OSL measurements on the basal marine sand units.

In the case of OSL 4, collected near the top of Group 1, the calculated age estimate appears to be too old but remains within error margins of the overlying and underlying samples. This sample was collected from a 4 cm thick carbonated sandy unit, just above a coarse sand containing common manganese concretions. Such features are indicative of post-depositional diagenetic changes and the modern field γ-ray spectroscopy measurements and laboratory-based determinations of radionuclide concentrations may therefore not enable the calculation of a reliable estimate of the true dose received by mineral grains throughout their burial time. This sample also provided one of the highest recorded water contents and it is possible that following the accumulation of fine

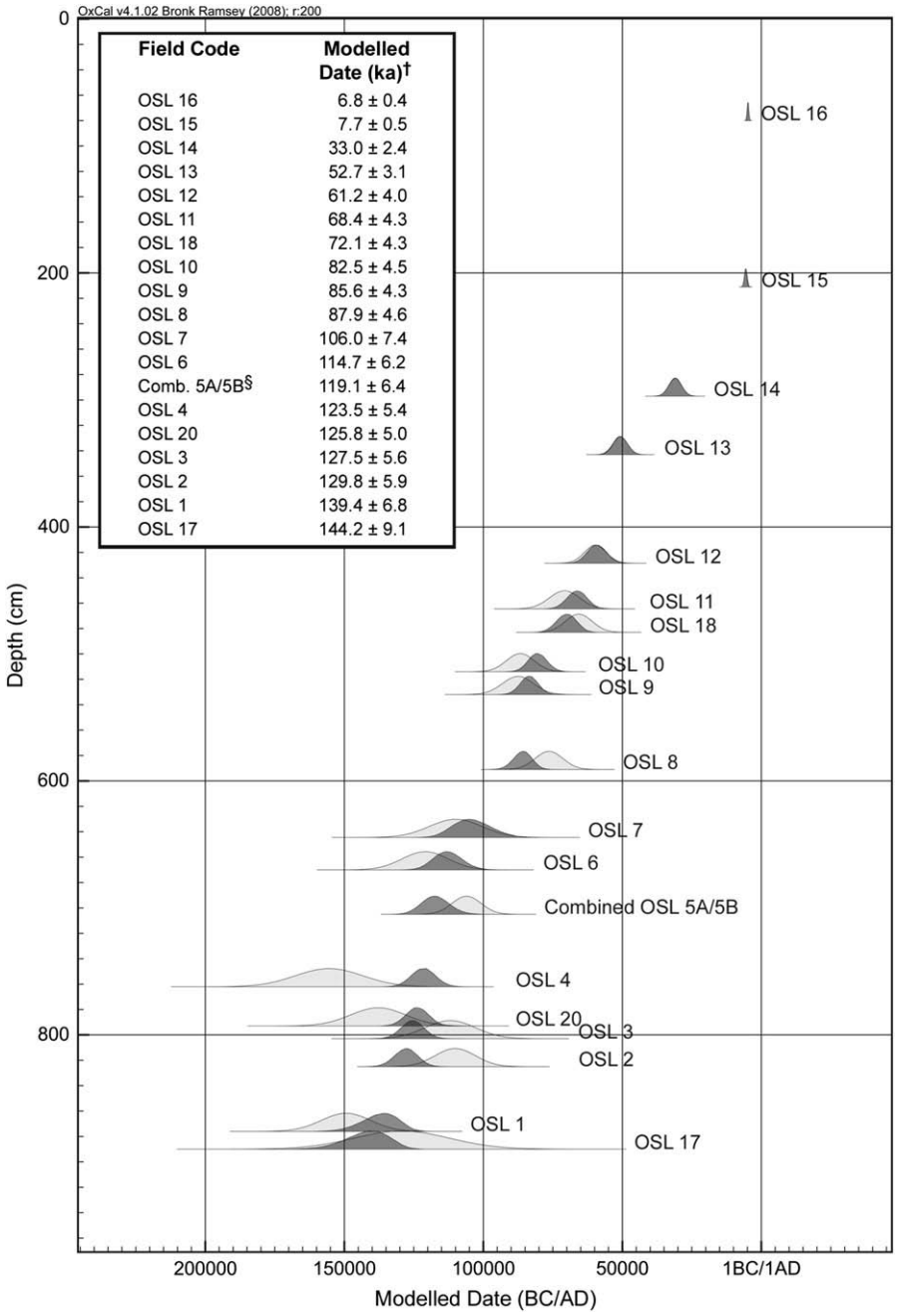

Fig. 9. Bayesian model of multi-grain dates for cave sediments, plotted by sample depth. The unmodelled dates are represented by light grey normal distributions, and the modelled dates by dark grey. The inset table gives the mean and error for the modelled dates. Notes: †Following Rhodes et al. (2003), water content error was removed from the dates before they were entered into the model. The uncertainty has been added back into the modelled dates for the values given here. §Since OSL 5A and OSL 5B were replicate samples, they have been treated as sub-samples of a single event in the model. The modelled, combined event date is presented in the figure and table.

carbonaceous particles at an unknown period in time, the water retention capability of the sediment could have been greatly enhanced thereby leading to an age overestimate.

Although, some degree of caution has to be ascertained regarding the precision of the dates obtained for the lowermost sediments there is little doubt as to their attribution to the marine high stand of the Last Interglacial. Despite potential difficulties with individual samples, the good characteristics of the luminescence signal of most of the cave sediments studied here as well as the consistent dates produced by the Bayesian analysis suggest that a reliable chronological framework of cave sedimentation and human occupation has been achieved.

6. Conclusions

Based on the OSL determinations and fresh assessment of the site's stratigraphy it is now clear that the human presence in the cave began soon after the marine high stand in G1 of our sequence, which on average can be dated to around 125 000 years ago. This presence can be documented by fresh-looking lithic artefacts and charcoal in sub-unit G1.7 and is most closely associated with OSL 2. It is important to note that the artefact-bearing deposits rest almost immediately on top of the marine beach which, as argued above, is identified with MIS 5.1. We are aware of course of the amino acid racemisation (AAR) differential between MIS 5 and 7 reported in

the Casablanca area (Occhietti et al., 2002) and given the excellent preservation of shell in the Group 1 sediments we intend to apply AAR dating in the future as an independent check on the age of this marine interval at DeS I, with biostratigraphy also promising a further set of tests for our current OSL age model.

Notwithstanding human activity at this early date it is difficult to attribute the artefacts specifically to the Aterian because of the absence of diagnostic tools. The first unambiguous evidence for the Aterian comes from the artefacts in Ruhlmann's Layer I which we correlate with our sub-units G2 (2–6) also confirmed by the discovery in 2005 of a typical pedunculate point in the section from within this part of the sequence. The artefacts in these sub-units can be dated by OSL 6 and are bracketed by dates provided by OSL 7 and OSL 5a and 5b. In combination these would place the oldest Aterian within the later stages of MIS 5, probably earlier than 110 000 years ago.

The consequences of accepting this new dating scheme are profound. First, the Aterian in the Atlantic area between Rabat and Témara was once considered to be represented only by its middle and late phases (Roche, 1969; Roche and Texier, 1976). It now seems that the technology is earlier than previously suspected in this part of Morocco and older too probably than in Tunisia and parts of the Libyan Sahara or on its northern fringes. Secondly, because of the associated presence of symbolic ornaments such as shell beads (Bouzouggar et al., 2007a) and other cultural novelties in the Aterian, it can be shown that such developments happened even earlier in North West Africa than has so far been demonstrated in more traditionally accepted centres of southern and eastern parts of the continent. This in turn suggests that a fuller re-appraisal is now required of the timing and interpretation of earliest behavioural innovations linked with the dispersal of modern humans. The occurrence of the Aterian in North West Africa in the later part of MIS 5 also challenges the notion that technological, ecological and social changes were principally a response to rapid climatic and environmental changes 80–70 000 years ago (Mellars, 2006). Our evidence would indicate that such developments began earlier and were not just restricted in their geographical spread to sub-Saharan Africa.

The implications of the new dating are not only far reaching for the human occupation of the region. As has already been noted, DeS I is the type site for the Soltanian but the boundary of this chronozone with the underlying Ouljian is still unresolved, even in MIS terms. Some authors place MIS 5.1–4 in the Ouljian (cf. Texier et al., 2002; Rhodes et al., 2006) whilst others leave these substages out altogether (cf. Occhietti et al., 2002). There would seem to be an equally strong argument for placing in the Soltanian what will usually be, in surviving exposures (including those at DeS I), 'continental' deposits.

In conclusion, the new OSL results have provided a much needed framework for resolving many of the chronostratigraphic questions left open by earlier research at this site and, in particular, in relation to identifying the timing of Aterian occupation in this region. Further work is already in progress and some of the preliminary dating results on nearby Aterian sites in the Témara area are largely in agreement with those of DeS I (Schwenninger et al., 2009). The generally very high quality of the stratigraphic, palaeoenvironmental and archaeological data in these caves (cf. Nespoulet et al., 2008) will allow a much better understanding of what we suspect will be the early part of the Aterian, and thus of emerging modern behaviour in humans, at least in this part of Africa.

Acknowledgements

The authors would like to thank the *Institut National des Sciences de l'Archéologie et du Patrimoine* (INSAP), and especially its director Professor Aomar Akerraz, for permission to work at Dar es-Soltan I. The EFCHED project paid for the logistics and dating work in 2005, while funding for the most recent fieldwork was provided under the RESET (Response of Humans to Abrupt Climatic Transitions) programme funded by NERC and the PROTARS project. Our thanks also go to Alison Wilkins and Ian Cartwright of the Institute of Archaeology for their help with the figures.

References

Adamiec, G., Aitken, M.J., 1998. Dose–rate conversion factors: new data. Ancient TL 16, 37–50.
Aitken, M.J., 1998. An Introduction to Optical Dating. Oxford University Press, Oxford.
Aitken, M.J., Smith, B.W., 1988. Optical dating: recuperation after bleaching. Quat. Sci. Rev. 7, 387–393.
Alimen, M.H., Beucher, F., Conrad, G., 1966. Chronologie du dernier cycle pluvial au Sahara nord-occidental. C. R. Acad. Sci. Paris 263, 5–8.
Antoine, M., 1937. Notes de préhistoire marocaine: XIII – La question atéro-ibéromaurusienne au Maroc: historique et mise au point. Bull. Soc. Préhist. Maroc. 11è année, 45–58.
Bar-Yosef, O., 2002. The Upper Palaeolithic revolution. Annu. Rev. Anthropol. 31, 363–393.
Barton, R.N.E., Bouzouggar, A., Bronk-Ramsey, C., Collcutt, S.N., Higham, T.F.G., Humphrey, L.T., Parfitt, S., Rhodes, E.J., Schwenninger, J.L., Stringer, C.B., Turner, E., Ward, S., 2007. Abrupt climatic change and chronology of the Upper Palaeolithic in northern and eastern Morocco. In: Mellars, P., Boyle, K., Bar-Yosef, O., Stringer, C. (Eds.), Rethinking the Human Revolution: New Behavioural & Biological Perspectives on the Origins and Dispersal of Modern Humans. Research Monographs of the Macdonald Institute, pp. 177–186. Cambridge.
Bateman, M.D., Holmes, P.J., Carr, A.S., Horton, B.P., Jaiswal, M.K., 2004. Aeolianite and barrier dune construction spanning the last two glacial–interglacial cycles from the southern Cape coast, South Africa. Quat. Sci. Rev. 23 (14–15), 1681–1698.
Berger, G.W., Pérez-González, A., Carbonell, E., Arsuaga, J.L., Bermúdez de Castro, J.-M., Ku, T.-L., 2008. Luminescence chronology of cave sediments at the Atapuerca paleoanthropological site, Spain. J. Hum. Evol. 55, 300–311.
Bordes, F., 1961. Typologie du Paléolithique ancien et moyen. Delmas, Bordeaux.
Bouzouggar, A., 1997a. Economie des matières premières et du débitage dans la séquence atérienne de la grotte d'El Mnasra I (ancienne grotte des Contrebandiers-Maroc). Préhist. Anthrop. Médit. (Aix-en-Prok-vence) 6, 35–52.
Bouzouggar, A., 1997b. Matières premières, processus de fabrication et de gestion des supports d'outils dans la séquence atérienne de la grotte d'El Mnasra I (ancienne grotte des Contrebandiers) à Témara (Maroc). Thèse de doctorat de l'Université Bordeaux I.
Bouzouggar, A., Barton, N., Vanhaeren, M., d'Errico, F., Collcutt, S., Higham, T., Hodge, E., Parfitt, S., Rhodes, E., Schwenninger, J.-L., Stringer, C., Turner, E., Ward, S., Moutmir, A., Stambouli, A., 2007a. 82,000 year-old shell beads from North Africa and implications for the origins of modern human behavior. Proc. Natl. Acad. Sci. U.S.A. 104 (24), 9964–9969.
Bouzouggar, A., Barton, R.N.E., De Araujo Igreja, 2007b. A brief overview of recent research into the Aterian and Upper Palaeolithic of Northern and Eastern Morocco. In: Barich, B. (Ed.), Tra il Sahara e il Mediterraneo: il Jebel Gharbi (Libia) e l'Archeologia del Maghreb. Edizioni Quasar. Scienze dell'Antichità, Storia Archeologia Antopologia 12 (2004–5), pp. 473–488.
Breuil, H., Frobenius, L., 1931. L'Afrique. Cahiers d'Art, Paris.
Bronk Ramsey, C., 1995. Radiocarbon calibration and analysis of stratigraphy: the OxCal Program. Radiocarbon 37, 425–430.
Bronk Ramsey, C., 2001. Development of the radiocarbon program OxCal. Radiocarbon 43, 355–363.
Brooke, B., 2001. The distribution of carbonate eolianite. Earth Sci. Rev. 55 (1–2), 135–164.
Brooke, B.P., Murray-Wallace, C.V., Woodroffe, C.D., Heijnis, H., 2003. Quaternary aminostratigraphy of eolianite on Lord Howe Island, Southwest Pacific Ocean. Quat. Sci. Rev. 22 (2–4), 387–406.
Carrière, G., 1886. Quelques stations préhistoriques de la Province d'Oran. Bull. Soc. Géog. Archéol. Oran VI, 136–154.
Caton-Thompson, G., 1946. The Aterian industry: its place and significance in the Palaeolithic world. J. R. Anthropol. Inst. G.B. Irel. 76 (2), 87–130.
Choubert, G., 1953. Les rapports entre les formations marines et continentales quaternaires. In: Actes du III è Congrès I.N.Q.U.A. Rome-Pise. pp. 576–590.
Choubert, G., Joly, F., Gigout, M., Marçais, J., Margat, J., Raynal, R., 1956. Essai de classification du Quaternaire continental du Maroc. C. R. Acad. Sci. Paris 243, 504–506.
Cremaschi, M., Di Lernia, S., Garcea, E.A.A., 1998. Some insights on the Aterian in the Libyan Sahara: chronology, environment, and archaeology. Afr. Archaeol. Rev. 15 (4), 261–286.
D'Errico, F., Henshilwood, C., 2007. Additional evidence for bone technology in the southern African Middle Stone Age. J. Hum. Evol. 52 (2), 142–163.
Debénath, A., 2000. Le peuplement préhistorique du Maroc: données récentes et problèmes. L'Anthropologie 104, 131–145.

Debénath, A., Raynal, J.-P., Texier, J.-P., 1982. Position stratigraphique des restes humains paléolithiques marocains sur la base des travaux récents. C. R. Acad. Sci. Paris, Sér. II 294, 1247–1250.
Debénath, A., Raynal, J.-P., Roche, J., Texier, J.-P., Ferembach, D., 1986. Stratigraphie, habitat, typologie at devenir de l'Atérien Marocain: Données récentes. L'Anthropologie 90 (2), 233–246.
Debruge, M.A., 1912. Les outils pédonculés de la Station Préhistorique de Aïn el Mouhaad, près Tebessa. In: VII Congrès Préhistorique Français, Angoulême. pp. 356–358.
Duller, G.A.T., 2004. Luminescence dating of Quaternary sediments: recent advances. J. Quat. Sci. 19, 183–192.
El Hajraoui, M.A., 1994. L'industrie osseuse atérienne de la grotte d'El Mnasra (Région de Témara,Maroc). LAPMO Université de Provence CNRS. Préhits. Anthrop. Médit. 3, 91–94.
Ferring, C.R., 1975. The Aterian in North African prehistory. In: Wendorf, F., Marks, A.E. (Eds.), Problems in Prehistory: North Africa and the Levant. Southern Methodist University Press, Dallas, pp. 113–126.
Frechen, M., Neber, A., Tsatskin, A., Boenigk, W., Ronen, A., 2004. Chronology of Pleistocene sedimentary cycles in the Carmel Coastal Plain of Israel. Quat. Int. 121 (1), 41–52.
Garcea, E.A.A., 2004. Crossing deserts and avoiding seas: Aterian North African–European relations. J. Anthropol. Res. 60, 27–53.
Garcea, E.A.A., Giraudi, C., 2006. Late Quaternary human settlement patterning in the Jebel Gharbi. J. Hum. Evol. 51, 411–421.
Hearty, P.J., Neumann, A.C., 2001. Rapid sea level and climate change at the close of the last interglaciation (MIS 5e): evidence from the Bahama Islands. Quat. Sci. Rev. 20 (18), 1881–1895.
Henderson, G.M., Robinson, L.F., Cox, K., Thomas, A.L., 2006. Recognition of non-Milankovitch sealevel highstands at 185 and 340 thousand years ago from U–Th dating of Bahamas sediment. Quat. Sci. Rev. 25 (23–24), 3346–3358.
Henshilwood, C., Marean, C.W., 2003. The origin of modern human behavior: critique of the models and their test implications. Curr. Anthropol. 44 (5), 627–649.
Henshilwood, C., D'Errico, F., Yates, R., Jacobs, Z., Tribolo, C., Duller, G.A., Mercier, N., Sealy, J., Valladas, H., Watts, I., Wintle, A., 2002. Emergence of modern human behavior: Middle Stone Age engravings from South Africa. Science 295, 1278–1280.
Hublin, J.-J., 1992. Recent human evolution in northwestern Africa. Philos. Trans. Biol. Sci. 337 (1280), 185–191.
Hublin, J.J., Bailey, S., Olejniczak, Smith, T., Verba, C., Sbihi-Alaoui, F., Zouak, M., 2007. Dental evidence from the Aterian human populations of Morocco. In: Modern Origins: a North African Perspective. 31st August–2nd September 2007. Max Planck Institute for Evolutionary Anthropology, Leipzig, Germany Abstracts: http://www.eva.mpg.de/evolution/conf2007/index.htm.
Huntley, D.J., Godfrey-Smith, D.I., Thewalt, M.L.W., 1985. Optical dating of sediments. Nature 313, 105–107.
Jacobs, Z., Duller, G.A.T., Wintle, A.G., 2003a. Optical dating of dune sand from Blombos Cave, South Africa: II—single grain data. J. Hum. Evol. 44, 613–625.
Jacobs, Z., Wintle, A.G., Duller, G.A.T., 2003b. Optical dating of dune sand from Blombos Cave, South Africa: I—multiple grain data. J. Hum. Evol. 44, 599–612.
Jacobs, Z., Duller, G.A.T., Wintle, A.G., Henshilwood, C.S., 2006. Extending the chronology of deposits at Blombos Cave, South Africa, back to 140 ka using optical dating of single and multiple grains of quartz. J. Hum. Evol. 51, 255–273.
Jacobs, Z., Roberts, R.G., Galbraith, R.F., Deacon, H.J., Grün, R., Mackay, A., Mitchell, P., Vogelsang, R., Wadley, L., 2008a. Ages for the Middle Stone Age of Southern Africa: implications for human behavior and dispersal. Science 322, 733–735.
Jacobs, Z., Wintle, A.G., Duller, G.A.T., Roberts, R.G., Wadley, L., 2008b. New ages for the post-Howiesons Poort, late and final Middle Stone Age at Sibudu, South Africa. J. Archaeol. Sci. 35, 1790–1807.
Lecointre, G., 1926. Recherches géologiques dans la Méséta marocaine. Mém. Soc. Sci. Nat. Maroc, Rabat 14, 1–158.
Lefèvre, D., Raynal, J.-P., 2002. Les formations plio-pléistocènes de Casablanca et la chronostratigraphie du quaternaire marin du Maroc revisitées. Quaternaire 13 (1), 9–21.
Lian, O., Roberts, R.G., 2006. Dating the Quaternary: progress in luminescence dating of sediments. Quat. Sci. Rev. 25, 2449–2468.
Martini, M., Sibilia, E., Zelaschi, C., Troja, S.O., Forzese, R., Gueli, A.M., Cro, A., Foti, F., 1998. TL and OSL dating of fossil dune sand in the Uan Afuda and Uan Tabu rockshelters, Tadrart Acacus (Libyan Sahara). In: Cremaschi, M., di Lernia, S. (Eds.), Wadi Teshuinat. Palaeoenvironment and Prehistory in South-Western Fezzan (Libyan Sahara). All'Insegna del Giglio, Firenze, pp. 67–72.
McBurney, C.B.M., 1967. The Haua Fteah (Cyrenaica) and the Stone Age of the South-East Mediterranean. Cambridge University Press, Cambridge.
McBrearty, S., Brooks, A.S., 2000. The revolution that wasn't: a new interpretation of the origin of modern human behavior. J. Hum. Evol. 39 (5), 453–563.
McLaren, S., 2007. Aeolianite. In: Nash, D.J., McLaren, S. (Eds.), Geochemical Sediments & Landscapes. Blackwell Publishing, Oxford, pp. 144–172.
Mejdahl, V., 1979. Thermoluminescence dating: beta-dose attenuation in quartz grains. Archaeometry 21, 61–72.
Mellars, P., 2006. Why did modern human populations disperse from Africa ca. 60,000 years ago? Proc. Natl. Acad. Sci. U.S.A. 103, 9381–9386.
Mercier, N., Wengler, L., Valladas, H., Joron, J.L., Froget, L., Reyss, J.-L., 2007. The Rhafas Cave (Morocco): chronology of the Mousterian and Aterian archaeological occupations and their implications for Quaternary geochronology based on luminescence (TL/OSL) age determinations. Quat. Geochron. 2, 309–313.
Moreau, F., 1888. Notices sur les silex taillés receuillis en Tunisie Paris.
Morgan, J., de Capitan, R., Boudy, P., 1910. Etudes sur les stations préhistoriques du Sud Tunisien. Rev. Ecol. Anthropol. 20.
Moura, D., Veiga-Pires, C., Albardeiro, L., Boski, T., Rodrigues, A.L., Tareco, H., 2007. Holocene sea level fluctuations and coastal evolution in the central Algarve (southern Portugal). Mar. Geol. 237 (3–4), 127–142.
Murray, A.S., Wintle, A.G., 2000. Luminescence dating of quartz using an improved single-aliquot regenerative-dose protocol. Radiat. Meas. 32, 57–73.
Murray-Wallace, C.V., 2002. Pleistocene coastal stratigraphy, sea-level highstands and neotectonism of the southern Australian passive continental margin – a review. J. Quat. Sci. 17 (5), 469–489.
Nespoulet, R., El Hajraoui, M.A., Amani, F., Ben-Ncer, A., Debénath, A., El Idrissi, A., Lacombe, J.-P., Michel, P., Oujaa, A., Stoetzel, E., 2008. Palaeolithic and Neolithic occupations in the Témara region (Rabat, Morocco): recent data on hominin contexts and behavior. Afr. Archaeol. Rev. 25 (1–2), 21–40.
Neuville, R., Ruhlmann, A., 1941. La place du paléolithique ancien dans le Quaternaire Marocain. Coll. Hespéris, Casablanca.
Nielsen, K.A., Clemmensen, L.B., Fornós, J.J., 2004. Middle Pleistocene magneto-stratigraphy and susceptibility stratigraphy: data from a carbonate aeolian system, Mallorca, Western Mediterranean. Quat. Sci. Rev. 23 (16–17), 1733–1756.
Occhietti, S., Raynal, J.-P., Pichet, P., Texier, J.-P., 1993. Aminostratigraphie du dernier cycle climatique au Maroc atlantique, de Casablanca à Tanger. C. R. Acad. Sci. Paris 317 (2), 1625–1632.
Occhietti, S., Raynal, J.-P., Pichet, P., Lefèvre, D., 2002. Aminostratigraphie des formations littorales pléistocènes et holocènes dans la région de Casablanca, Maroc. Quaternaire 13 (1), 55–64.
Ortiz, J.E., Torres, T., Yanes, Y., Castillo, C., De La Nuez, J., Ibáñez, M., Alonso, M.R., 2005. Climatic cycles inferred from the aminostratigraphy and amino-chronology of Quaternary dunes and palaeosols from the eastern islands of the Canary Archipelago. J. Quat. Sci. 21 (3), 287–306.
Osborne, A.H., Vance, D., Rohling, E., Barton, N., Rogerson, M., Fello, N., 2008. A humid corridor across the Sahara for the migration "out of Africa" of early modern humans 120,000 years ago. Proc. Natl. Acad. Sci. U.S.A. 105 (43), 16444–16447.
Plaziat, J.-C., Aberkan, M., Reyss, J.-L., 2006. New late Pleistocene seismites in a shoreline series including eolianites, north of Rabat (Morocco). Bull. Soc. Géol. Fr. 177 (6), 323–332.
Porat, N., Wintle, A.G., Ritte, M., 2004. Mode and timing of kurkar and hamra formation, central coastal plain, Israel. Isr. J. Earth Sci. 53 (1), 13–25.
Potter, E.-K., Esat, T.M., Schellmann, G., Radtke, U., Lambeck, K., McCulloch, M.T., 2004. Suborbital-period sea-level oscillations during marine isotope substages 5a and 5c. Earth Planet. Sci. Lett. 225, 191–204.
Prescott, J.R., Hutton, J.T., 1994. Cosmic ray contributions to dose rates for luminescence and ESR dating: large depths and long-term time variations. Radiat. Meas. 23, 497–500.
Prideaux, G.J., Long, J.A., Ayliffe, L.K., Hellstrom, J.C., Pillans, B., Boles, W.E., Hutchinson, M.N., Roberts, R.G., Cupper, M.L., Arnold, L.J., Devine, P.D., Warburton, N.M., 2007. An arid-adapted middle Pleistocene vertebrate fauna from south-central Australia. Nature 445, 422–425.
Reygasse, M., 1919–1920. Etudes de Palethnologie Maghrébine (Nouvelle série). Rec. Not. Mém. Soc. Archeol. Constantine LIII.
Rhodes, E.J., Schwenninger, J.-L., 2007. Dose rates and radioisotope concentrations in the concrete calibration blocks at Oxford. Ancient TL 25, 5–8.
Rhodes, E.J., Bronk Ramsey, C., Outram, Z., Batt, C., Willis, L., Dockrill, S., Bond, J., 2003. Bayesian methods applied to the interpretation of multiple OSL dates: high precision sediment ages from Old Scatness Broch excavations, Shetland Isles. Quat. Sci. Rev. 22 (10), 1231–1244.
Rhodes, E.J., Singarayer, J.S., Raynal, J.-P., Westaway, K.E., Sbihi-Alaoui, F.Z., 2006. New age estimates for the Palaeolithic assemblages and Pleistocene succession of Casablanca, Morocco. Quat. Sci. Rev. 25 (19–20), 2569–2585.
Roche, J., 1956. Etude sur l'industrie de la grotte de Dar-es-Soltane (Rabat). Bull. Archéol. Maroc. 1, 93–118.
Roche, J., 1963. L'Epipaléolithique Marocain. Fondation Calouste Gulbenkian, Lisbon.
Roche, J., 1969. Fouilles de la grotte des Contrebandiers (Maroc). Palaeoecol. Afr. 4, 120–121.
Roche, J., 1976. Cadre chronologique de l'Epipaléolithique marocain. In: Actes du IXè Congrès de l'UISPP, Nice, Colloque II: Chronologie et synchronisme dans la préhistoire circum-méditerranéenne. pp. 153–167.
Roche, J., Texier, J.-P., 1976. Découverte de restes humains dans un niveau atérien de la grotte des Contrebandiers à Témara, Maroc. C. R. Acad. Sci. Paris 282, 45–47.
Roset, J.-P., 2005. El-Akarit et le Paléolithique moyen en Tunisie. In: Archéologies, 20 ans de recherches françaises dans le monde, Edit. ADPF, Ministère des Affaires étrangères. pp. 225–226.
Ruhlmann, A., 1936. Les grottes préhistoriques d' "El Khenzira" (région de Mazagan). In: Publications du Service des Antiquités du Maroc, Rabat. Fasc. 2, pp. 103–105.
Ruhlmann, A., 1939. Recherches de préhistoire dans l'extrême-Sud marocain. In: Publications du Service des Antiquités du Maroc, Rabat. Fasc. 5, pp. 1–108.
Ruhlmann, A., 1951. La grotte préhistorique de Dar es-Soltan. In: Collection Hésperis 11. Institut des Hautes Études Marocaines, Larose, Paris, pp. 1–210.
Schellmann, G., Radtke, U., Potter, E.-K., Esat, T.M., McCulloch, M.T., 2004. Comparison of ESR and TIMS U/Th dating of marine isotope stage (MIS) 5e, 5c, and 5a coral from Barbados – implications for palaeo sea-level changes in the Caribbean. Quat. Int. 120, 41–50.

Schwenninger, J.-L., Collcutt, S.N., Barton, R.N.E., Bouzouggar, A., El Hajraoui, M.A., Nespoulet, R., Debénath, A., 2009. Luminescence chronology for Aterian cave sites on the Atlantic coast of Morocco. In Garcea, E.E.A. (ed), South-Eastern Mediterranean Peoples between 130,000 and 10,000 Years Ago. Oxbow Books, Oxford.

Siddall, M., Rohling, E.J., Almogi-Labin, A., Hemleben, C., Meischner, D., Schmelzer, I., Smeed, D.A., 2003. Sea-level fluctuations during the last glacial cycle. Nature 423, 853–858.

Siddall, M., Chappell, J., Potter, E.-K., 2007. Eustatic sea level during past interglacials. In: Sirocko, F., Claussen, M., Sanchez-Goni, M.-F., Litt, T. (Eds.), The Climate of Past Interglacials. Developments in Quaternary Science Series No. 7. Elsevier, Amsterdam, pp. 75–92.

Smith, J.R., Hawkins, A.L., Asmerom, Y., Polyak, V., Giegengack, R., 2007. New age constraints on the Middle Stone Age occupations of Kharga Oasis, Western Desert, Egypt. J. Hum. Evol. 52 (6), 690–701.

Szabo, B.J., Haynes, C.V., Maxwell, T.A., 1995. Ages of Quaternary pluvial episodes determined by uranium-series and radiocarbon dating of lacustrine deposits of Eastern Sahara. Palaeogeogr. Palaeoclimatol. Palaeoecol. 113 (2–4), 227–242.

Texier, J.-P., Huxtable, J., Rhodes, E., Miallier, D., Ousmoi, M., 1988. Nouvelles données sur la situation chronologique de l'Atérien du Maroc et leurs implications. C. R. Acad. Sci. Paris, Ser. II 307, 827–832.

Texier, J.-P., Lefèvre, D., Raynal, J.-P., El Graoui, M., 2002. Lithostratigraphy of the littoral deposits of the last one million years in the Casablanca region (Morocco). Quaternaire 13 (1), 23–41.

Thompson, W.G., Goldstein, S.L., 2005. Open-system coral ages reveal persistent suborbital sea-level cycles. Science 308, 401–404.

Tillet, T., 1995. Recherches sur l'Atérien du Sahara méridional (bassins Tchadien et de Taoudenni): position chrono-stratigraphique, définition et étude comparative. In: Chenorkian, R. (Ed.), L'homme méditerranéen. Mélanges offerts à Gabriel Camps. Publications de l'Université de Provence, Aix-en-Provence, pp. 29–56.

Trinkaus, E., 2007. European early modern humans and the fate of the Neandertals. Proc. Natl Acad. Sci. U.S.A. 104, 7367–7372.

Van Peer, P., 1998. The Nile corridor and the out-of-Africa model: an examination of the archeological records. Curr. Anthropol. (Suppl. 39), S115–S140.

Wadley, L., 2001. What is cultural modernity? A general view and a South African perspective from Rose Cottage Cave. Camb. Archaeol. J. 11 (2), 201–221.

Watson, E., Forster, P., Richards, M., Bandelt, H.-J., 1997. Mitochondrial footprints of human expansion in Africa. Am. J. Hum. Genet. 61, 691–704.

Wengler, L., 1993. Formations quaternaires et cultures préhistoriques au Maroc oriental. Thèse de Doctorat d'État à l'Université Bordeaux I, France.

Wrinn, P.J., Rink, W.J., 2003. ESR dating of tooth enamel from Aterian levels at Mugharet el 'Aliya (Tangier, Morocco). J. Archaeol. Sci. 30, 123–133.

Zazo, C., Goy, J.L., Hillate-Marcel, C., Lario, J., Dabrio, C.J., Hoyos, M., Bardaji, T., Silva, P.G., Somoza, L., 2000. The record of highstand sea-level during the last interglacials (isotope stages 7, 5 and 1) in the Atlantic–Mediterranean linkage area. In: Finlayson, C., Finlayson, G., Fa, D. (Eds.), Gibraltar During the Quaternary. Monograph 1. Gibraltar Government Heritage Publications, pp. 87–92.

Zimmerman, D.W., 1971. Thermoluminescent dating using fine grains from pottery. Archaeometry 13, 29–50.